



Heterologous Production of Glycine Betaine Using *Synechocystis* sp. PCC 6803-Based Chassis Lacking Native Compatible Solutes

Eunice A. Ferreira^{1,2,3}, Catarina C. Pacheco^{1,2}, João S. Rodrigues^{1,2,4†}, Filipe Pinto^{1,2}, Pedro Lamosa⁵, David Fuente⁶, Javier Urchueguía⁶ and Paula Tamagnini^{1,2,4*}

OPEN ACCESS

Edited by:

Shota Atsumi,
University of California, Davis,
United States

Reviewed by:

Xuefeng Lu,
Qingdao Institute of Bioenergy and
Bioprocess Technology (CAS), China
Jianping Yu,
National Renewable Energy
Laboratory (DOE), United States
Weiwen Zhang,
Tianjin University, China

*Correspondence:

Paula Tamagnini
pmtamagn@ibmc.up.pt

†Present Address:

João S. Rodrigues,
Department of Chemistry—Ångström,
Uppsala University, Uppsala, Sweden

Specialty section:

This article was submitted to
Synthetic Biology,
a section of the journal
Frontiers in Bioengineering and
Biotechnology

Received: 23 November 2021

Accepted: 15 December 2021

Published: 07 January 2022

Citation:

Ferreira EA, Pacheco CC,
Rodrigues JS, Pinto F, Lamosa P,
Fuente D, Urchueguía J and
Tamagnini P (2022) Heterologous
Production of Glycine Betaine Using
Synechocystis sp. PCC 6803-Based
Chassis Lacking Native
Compatible Solutes.
Front. Bioeng. Biotechnol. 9:821075.
doi: 10.3389/fbioe.2021.821075

¹IS—Instituto de Investigação e Inovação em Saúde, Universidade do Porto, Porto, Portugal, ²IBMC—Instituto de Biologia Molecular e Celular, Universidade do Porto, Porto, Portugal, ³ICBAS—Instituto de Ciências Biomédicas Abel Salazar, Universidade do Porto, Porto, Portugal, ⁴Departamento de Biologia, Faculdade de Ciências, Universidade do Porto, Porto, Portugal, ⁵Instituto de Tecnologia Química e Biológica António Xavier, ITQB NOVA, Oeiras, Portugal, ⁶Instituto de Aplicaciones de las Tecnologías de la Información y de las Comunicaciones Avanzadas, Universitat Politècnica de València, València, Spain

Among compatible solutes, glycine betaine has various applications in the fields of nutrition, pharmaceuticals, and cosmetics. Currently, this compound can be extracted from sugar beet plants or obtained by chemical synthesis, resulting in low yields or high carbon footprint, respectively. Hence, in this work we aimed at exploring the production of glycine betaine using the unicellular cyanobacterium *Synechocystis* sp. PCC 6803 as a photoautotrophic chassis. *Synechocystis* mutants lacking the native compatible solutes sucrose or/and glucosylglycerol— Δsps , $\Delta ggpS$, and $\Delta sps\Delta ggpS$ —were generated and characterized. Under salt stress conditions, the growth was impaired and accumulation of glycogen decreased by ~50% whereas the production of compatible solutes and extracellular polymeric substances (capsular and released ones) increased with salinity. These mutants were used as chassis for the implementation of a synthetic device based on the metabolic pathway described for the halophilic cyanobacterium *Aphanothece halophytica* for the production of the compatible solute glycine betaine. Transcription of ORFs comprising the device was shown to be stable and insulated from *Synechocystis*' native regulatory network. Production of glycine betaine was achieved in all chassis tested, and was shown to increase with salinity. The introduction of the glycine betaine synthetic device into the $\Delta ggpS$ background improved its growth and enabled survival under 5% NaCl, which was not observed in the absence of the device. The maximum glycine betaine production [64.29 $\mu\text{mol/gDW}$ (1.89 $\mu\text{mol/mg protein}$)] was reached in the $\Delta ggpS$ chassis grown under 3% NaCl. Taking into consideration this production under seawater-like salinity, and the identification of main key players involved in the carbon fluxes, this work paves the way for a feasible production of this, or other compatible solutes, using optimized *Synechocystis* chassis in a pilot-scale.

Keywords: compatible solutes, cyanobacteria, glycine betaine, glucosylglycerol, salt stress, sucrose, *Synechocystis*, synthetic biology

Abbreviations: CPS, capsular polysaccharides; CS, compatible solutes; DW, dry weight; EPS, extracellular polymeric substances; FW, fresh weight; GB, glycine betaine; GG, glucosylglycerol; NMR, nuclear magnetic resonance; RPS, released polysaccharides; RT-qPCR, reverse transcription quantitative PCR.

INTRODUCTION

Microorganisms can cope with environmental stresses such as temperature, salinity or drought via the production of compatible solutes (CS)—low-molecular weight organic compounds highly soluble in water that can accumulate intracellularly up to molar concentrations, without interfering with the cell metabolism (Klähn and Hagemann, 2011). CS belong to different chemical classes including sugars (e.g., sucrose, trehalose), polyols (e.g., glycerol, sorbitol), heterosides (e.g., glucosylglycerol, floridoside), and amino acids or their derivatives (e.g., proline, glutamate, glycine betaine, ectoine) (Kirsch et al., 2019). Glycine betaine (or *N,N,N*-trimethylglycine) is an ubiquitous solute that can be found in bacteria, plants and mammals, being mostly synthesized by the two-step oxidation of choline to betaine aldehyde and subsequently to glycine betaine (Landfald and Strøm, 1986; Grossman and Hebert, 1989; Rathinasabapathi et al., 1997). Later on, the synthesis of glycine betaine *via* a three-step methylation of glycine was described in extremely halophilic bacteria (Nyyssola et al., 2000; Waditee et al., 2003). This biosynthetic pathway involves two *N*-methyltransferases: the glycine-sarcosine-*N*-methyltransferase (GSMT) that catalyzes the methylation of glycine and sarcosine, and the dimethylglycine-*N*-methyltransferase (DMT) that converts dimethylglycine to glycine betaine. This CS has a strong stabilizing effect on biomolecules, by maintaining their structure and function (Guinn et al., 2011; Stadtmiller et al., 2017), and thus conferring drought-, osmo- and thermo-protection to cells (Caldas et al., 1999; Holmström et al., 2000; Cleland et al., 2004; You et al., 2019). Moreover, glycine betaine plays an important physiological role as methyl group donor with beneficial stress-mitigating effects in humans (Lever and Slow, 2010; Day and Kempson, 2016), and up-regulating antioxidant defense systems in plants (Rady et al., 2018; Sun et al., 2020). Due to these interesting properties, glycine betaine is a value-added compound with applications in human nutrition, animal feed, agriculture, pharmaceuticals, and cosmetics (Eklund et al., 2005; Lever and Slow, 2010; Nsimba et al., 2010; Cholewa et al., 2014; Day and Kempson, 2016; Dikilitas et al., 2020). Most of the commercially available glycine betaine is extracted from sugar beets (*Beta vulgaris*) (Heikkilä et al., 1982), resulting in relatively low yields and rendering this organic production an expensive process. Alternatively, glycine betaine can be produced by chemical synthesis, but this process, although cheaper, has a high environmental impact increasing the carbon footprint (DuPont, 2015; Kar et al., 2015). A more sustainable and cost-effective production is highly desirable, and thus cyanobacteria emerge as promising chassis for the production of compatible solutes and other products of interest. Their photoautotrophic metabolism enables the sequestration and conversion of atmospheric CO₂ into organic compounds using sunlight and water as energy and electron sources, respectively (Knoll, 2008; Ananya and Ahmad, 2014). Therefore, they are being increasingly

studied to be used as solar-powered cell factories for many biotechnological applications including the production of e.g., alcohols, alkanes, hydrogen, sugars, and terpenoids (Hays and Ducat, 2015; Lindblad, 2018; Sadvakasova et al., 2020; Wang et al., 2020; Rodrigues and Lindberg, 2021). Among cyanobacteria, the unicellular *Synechocystis* sp. PCC 6803 (hereafter *Synechocystis*) is the best studied strain, and the vast array of data generated over the past decades allowed the construction of genome-scale metabolic models to predict system's behavior (Montagud et al., 2010; Montagud et al., 2011; Joshi et al., 2017; Gopalakrishnan et al., 2018). Moreover, various molecular and synthetic biology tools are now available for the genetic manipulation and engineering of this particular cyanobacterial strain (Huang et al., 2010; Heidorn et al., 2011; Pinto et al., 2015; Pacheco et al., 2021). *Synechocystis* is a freshwater strain and thus moderately halotolerant, relying on the biosynthesis of the compatible solutes sucrose, glutamate and glucosylglycerol to maintain the osmotic pressure under stress conditions (Klähn and Hagemann, 2011; Iijima et al., 2020).

In this study, *Synechocystis* knockout mutants in the biosynthetic pathways producing the main native compatible solutes sucrose or/and glucosylglycerol were generated to serve as chassis for the production of value-added compounds. The genome-scale metabolic model *iSyn811* was used to simulate the production rates of different heterologous CS and the highest rate was predicted for glycine betaine. As a proof-of-concept, we explored the production of this compatible solute using our *Synechocystis*-based chassis. For this purpose, a synthetic device based on the biosynthetic gene cluster from the halophilic cyanobacterium *Aphanothece halophytica* was constructed and introduced in the different chassis. Besides showing the production of glycine betaine and validating the functionality of the synthetic device, the characterization of the strains contributes to a better understanding of the mechanisms used by the cells to maintain homeostasis and cope with different levels of salinity.

MATERIALS AND METHODS

Reagents and Enzymes

The media components and other reagents were obtained from Fisher Scientific (United States), Merck (Germany) or Sigma Aldrich (United States), and noble agar from Difco (United States). All DNA-modifying enzymes and polymerases were purchased from Thermo Fisher Scientific (United States) and Promega (United States), and standard molecular biology kits were obtained from NZY Tech (Portugal). The Sanger sequencing and oligo synthesis services were provided by STAB VIDA, Lda (Portugal).

Organisms and Culture Conditions

Wild-type and mutants of the unicellular, non-motile cyanobacterium *Synechocystis* sp. PCC 6803 substrain GT-Kazusa (Kanesaki et al., 2012; Trautmann et al., 2012)

(obtained from the Pasteur Culture Collection, France) were maintained in Erlenmeyer flasks batch cultures with BG11 medium (Stanier et al., 1971) at 30°C with orbital shaking (150 rpm) under a 12 h light/12 h dark regimen. Light intensity was 25 $\mu\text{E}/\text{m}^2/\text{s}$ in all experiments and Cosine-corrected irradiance was measured using a Dual Solar/Electric Quantum Meter (Spectrum Technologies, Inc., United States). For solid BG11, the medium was supplemented with 1.5% (wt/vol) noble agar, 0.3% (wt/vol) sodium thiosulfate and 10 mM TES-KOH buffer, pH 8.2 (Stanier et al., 1971). For the selection and maintenance of mutants, BG11 medium was supplemented with chloramphenicol (Cm, 10–20 $\mu\text{g}/\text{ml}$). For cloning purposes, *E. coli* strains DH5 α and XL1-blue were used. Cells were grown at 37°C in LB medium (Sambrook and Russel, 2001), supplemented with kanamycin (Km, 50 $\mu\text{g}/\text{ml}$) or Cm (34 $\mu\text{g}/\text{ml}$).

DNA and RNA Extraction

Cyanobacterial genomic DNA (gDNA) extraction was performed according to the procedure described previously (Tamagnini et al., 1997). For RNA extraction, 50 ml of *Synechocystis* culture at $\text{OD}_{730} \approx 1$ was centrifuged for 10 min at 4,470 g; cell pellets were treated with RNeasy Protect Bacteria Reagent (Qiagen, Germany) according to instructions, and stored at -80°C . RNA was extracted using the TRIzol[®] Reagent (Ambion) according to the method described previously (Leitão et al., 2006) with the following adaptations: the cells were disrupted using a FastPrep[®]-24 (MP Biomedicals) in 2 cycles of 1 min at 4.0 m/s and the RNA samples were treated with 1 U of RQ1 RNase-Free DNase (Promega) according to manufacturer's instructions.

Glycine Betaine Device: Design, DNA Synthesis, and Assembly

The synthetic construction for the synthesis of glycine betaine (Ahbet) was designed based on *gsmt* (encoding the glycine-sarcosine-*N*-methyltransferase) and *dmt* (encoding the dimethylglycine-*N*-methyltransferase) Open Reading Frames (ORFs) from the cyanobacterium *Aphanothece halophytica*, and the *metX* (*sll0927*, encoding *S*-adenosyl-methionine synthase) ORF from *Synechocystis*. All the ORF sequences were codon optimized for *Synechocystis* using the Gene Designer 2.0 software (DNA 2.0, Inc., United States), restriction sites incompatible with the BioBrick[™] standard RFC [10] were eliminated and double stop codons included. Each ORF is preceded by the BioBrick[™] (BB) ribosome binding site (RBS) BBa_B0030 and the double terminator BBa_B0015 was included after the *metX* ORF. In addition, the synthetic construction is flanked by the prefix and suffix sequences of the BB RFC [10] standard. All the BB sequences were retrieved from the Registry of Standard Biological Parts (parts.igem.org). Subsequently, the sequence of the glycine betaine synthetic construction flanked by the BB prefix, the double terminator and BB suffix was synthesized and cloned into *Sma*I digested pBluescript II SK(-) (Epoch Life Science, Inc., United States).

To construct the glycine betaine device, the synthesized Ahbet construct was assembled with the synthetic promoter $P_{trc.x.lacO}$, previously characterized in *Synechocystis* (Ferreira et al., 2018). For this purpose, the Ahbet was PCR-amplified from the plasmid pBSK with the pUC primers (Additional file 1: **Supplementary Table S4**), using Phusion high-fidelity DNA polymerase, according to the manufacturer's instructions. The PCR product was purified using NZYGelpure kit, digested with *Xba*I and *Pst*I and cloned downstream of $P_{trc.x.lacO}$ in the pJ201 plasmid (digested with *Spe*I and *Pst*I, and dephosphorylated). The generated $P_{trc.x.lacO}::\text{Ahbet}$ device was excised from the pJ201 plasmid with *Xba*I and *Spe*I, and transferred to pSEVA351 shuttle vector (Silva-Rocha et al., 2013), digested with *Xba*I. The pSEVA351 was obtained from the "Standard European Vector Architecture" repository and is comprised by the broad-host-range replicon RSF1010 and the chloramphenicol antibiotic marker. The assembly and transfer of the synthetic device was confirmed by PCR, restriction analysis and Sanger sequencing.

Construction of Integrative Plasmids for the Generation of CS Mutants

The construction of integrative plasmids for the knockout of *ggpS* (glucosylglycerol-phosphate synthase) and *sps* (sucrose-phosphate synthase) genes was performed as described previously (Pinto et al., 2012). Briefly, the plasmids were based on pGEM-T[®] Easy (Promega, United States) and contain the *Synechocystis* chromosomal regions flanking the *ggpS* or the *sps* gene. The 5'- and 3'-flanking regions were amplified from the cyanobacterium's genome using *Pfu* DNA polymerase and the primer pairs 5-O/5-I and 3-O/3-I (Additional file 1: **Supplementary Table S4**), respectively. Subsequently, the purified PCR fragments were fused by Overlap Extension PCR using primers 5-O/3-O and 80 ng of each amplicon. The resulting product was purified and cloned into the vector pGEM-T[®] Easy, according to the manufacturer's instructions, originating the pGDggpS, and the pGDsps plasmids (**Table 1**). A selection cassette, containing the *nptII* gene (conferring resistance to neomycin and kanamycin) and the *sacB* gene (conferring sensitivity to sucrose), was PCR amplified from the plasmid pK18mobsacB (Schafer et al., 1994) with specific primers (Additional file 1: **Supplementary Table S4**). The amplicon was then cloned into the *Age*I/*Sma*I restriction site of pGDggpS or pGDsps plasmids, generating the pGDggpS.KS and the pGDsps.KS plasmids, respectively (**Table 1**). All constructs were confirmed by sequencing.

Generation of *Synechocystis* CS Knockout Mutants

Synechocystis was transformed based on the protocol described by Williams (1988) with modifications. *Synechocystis* cultures were grown under standard conditions to an $\text{OD}_{730} \approx 0.5$. Cells were harvested by centrifugation at 3,850 g for 10 min; and then resuspended in BG11 to a final $\text{OD}_{730} \approx 2.5$. A 500 μL aliquot of these cells was used (per transformation) and incubated with

TABLE 1 | List of plasmids used to transform *Synechocystis*.

| Designation | Plasmid | Description | Reference/Source |
|---------------------------------|--------------|---|------------------------|
| P _{trc.x.lacO} ::Ahbet | pSEVA351 | Ahbet synthetic construction under the control of the P _{trc.x.lacO} promoter | This study |
| pGDgppS | pGEM-T® Easy | pGEM-T easy vector containing the two regions for double homologous recombination targeting the <i>gppS</i> locus | Ferreira et al. (2018) |
| pGDgppS.KS | pGEM-T® Easy | pGEM-T easy vector containing the <i>nptII</i> and <i>sacB</i> genes flanked by the two regions for double homologous recombination targeting the <i>gppS</i> locus | This study |
| pGDsps | pGEM-T® Easy | pGEM-T easy vector containing the two regions for double homologous recombination targeting the <i>sps</i> locus | This study |
| pGDsps.KS | pGEM-T® Easy | pGEM-T easy vector containing the <i>nptII</i> and <i>sacB</i> genes flanked by the two regions for double homologous recombination targeting the <i>sps</i> locus | This study |

purified pGDgppS.KS or pGDsps.KS plasmids, at a final DNA concentration of 20 µg/ml, for 5 h in light at 30°C. Cells were then spread onto Immobilon™-NC membranes (0.45 µm pore size, 82 mm, Millipore, United States) resting on solid BG11 plates, incubated at 25°C under low light, and transferred to selective solid BG11 plates supplemented with 10 µg/mL Km after 24 h. Transformants were observed after 1–2 weeks. For complete segregation, Km-resistant colonies were streaked on BG11 plates with increasing Km concentrations (up to 500 µg/ml), and finally transferred into liquid medium. Mutants were then tested for sucrose sensitivity and confirmed by PCR and Southern blot (for details see below). Subsequently, to remove the selection markers from the insertion mutants, cells were transformed as described above with the pGDgppS or the pGDsps plasmids, and the mutants were selected on solid BG11 containing 10% (wt/vol) sucrose. These mutants were also screened for Km-sensitivity. The double mutant Δ sps Δ gppS was generated by deleting the *gppS* gene from the Δ sps background following the abovementioned protocol. The full segregation of the mutants was confirmed by PCR using GoTaq® G2 Flexi DNA Polymerase, together with specific primers (Additional file 1: **Supplementary Table S4**), according to manufacturer's instructions. Mutant segregation was also confirmed by Southern blots that were performed using 4 µg of genomic DNA of the wild-type and mutants, digested with *MunI* (wild-type, Δ sps.KS, Δ sps, Δ gppS.KS, and Δ gppS), and *AvaII* (wild-type, Δ sps Δ gppS.KS, and Δ sps Δ gppS). The DNA fragments were separated by electrophoresis on a 1% (wt/vol) agarose gel and blotted onto Hybond™-N membrane (GE Healthcare, United States). Probes covering the 5' flanking region of the *gppS* or 3' flanking region of the *sps* genes were amplified by PCR (using primers indicated in Additional file 1: **Supplementary Table S4**), and labeled using the DIG DNA labelling kit (Roche Diagnostics GmbH, Germany), according to the manufacturer's instructions. Hybridization was performed overnight at 65°C, and digoxigenin-labelled probes were detected by chemiluminescence using CPD-star (Roche) in a Chemi Doc™ XRS+ Imager (Bio-Rad, United States).

Introduction of the Glycine Betaine Synthetic Device Into *Synechocystis*

The pSEVA351 plasmid containing the synthetic device P_{trc.x.lacO}::Ahbet (Table 1; sequence provided in

Supplementary Datasheet S2) was introduced into *Synechocystis* by electroporation following the protocol described previously (Ferreira et al., 2018). The presence of the synthetic device was confirmed in *Synechocystis* transformants by PCR using specific primers (Additional file 1: **Supplementary Table S4**), as described by Ferreira et al. (2018).

Growth Experiments

Pre-cultures of *Synechocystis* wild-type and mutants were inoculated in BG11 medium (supplemented with 10 µg/ml Cm, when appropriate) and grown in an orbital shaker (150 rpm), at 30°C under a 12 h light (25 µE/m²/s)/12 h dark regimen. The cultures were grown to an OD₇₃₀ ≈ 2 and, subsequently, diluted in fresh BG11 medium without antibiotic to a final OD₇₃₀ ≈ 0.5. Fifty milliliters of the dilution were transferred to 100 ml Erlenmeyer flasks without NaCl or containing 3, 5, or 7% (wt/vol) NaCl (510, 860, and 1,200 mM NaCl, respectively), previously sterilized. These cultures were maintained in the same conditions as the pre-cultures and growth was monitored for at least 16 days, by measuring the optical density at 730 nm (OD₇₃₀) and determining the chlorophyll *a* (chl *a*) content as described by Meeks and Castenholz (1971). All the growth experiments included, at least, three biological replicates with technical duplicates.

Total Carbohydrate Content, Released and Capsular Polysaccharides Measurements

Total carbohydrate content and RPS were determined as previously described (Mota et al., 2013). Briefly, 10 ml of culture samples were dialyzed (12–14 kDa molecular weight cutoff; CelluSepT4, Orange Scientific) against at least 10 volumes of distilled water, 3 or 5% (wt/vol) NaCl solutions (identical to the growth medium), for at least 24 h. One milliliter of the collected sample was used to spectrophotometrically quantify the total carbohydrate content by the phenol-sulfuric acid method (Dubois et al., 1956), whereas 5 ml of the dialyzed sample was centrifuged at 3,857 g for 10 min at RT, and the cell-free supernatant was used to determine the RPS. For CPS quantification, the procedure was performed as described previously (Pereira et al., 2019). Five milliliters of

dialyzed cultures were centrifuged at 3,857 g for 10 min at RT, the cell pellet was resuspended in water and boiled for 15 min. After centrifugation as described previously, the cell-free supernatant was used for CPS measurement by the phenol-sulfuric acid method (Dubois et al., 1956). Total carbohydrate content, RPS and CPS were normalized by chl *a* content. All experiments included, at least, three biological replicates with technical triplicates.

Glycogen Extraction and Quantification

Glycogen extraction was performed as described previously (Ernst et al., 1984). Ten milliliters of cell culture were collected 1 h after the transition between the dark and the light phase. Samples were centrifuged, and the cell pellets suspended in 100 μ L of distilled water and 400 μ L of 30% (wt/vol) KOH was added. The mixture was incubated at 100°C for 90 min and then quickly cooled on ice. Six hundred μ L of ice-cold absolute ethanol were added, and the mixture was incubated on ice for 2 h. The mixture was centrifuged for 5 min at maximum speed and 4°C. The supernatant was discarded, and the isolated glycogen was washed three times with 500 μ L of ice-cold absolute ethanol and dried at 60°C. Glycogen quantification was performed by the phenol-sulfuric acid method (Dubois et al., 1956), and normalized by chl *a* content. Experiments included, at least, three biological replicates with technical triplicates.

Optical Microscopy

Cultures of *Synechocystis* wild-type (WT) and the Δ *sps* mutant were grown in BG11 or BG11 supplemented with 5% (wt/vol) NaCl as stated above (initial OD₇₃₀ \approx 0.5). Four days after inoculation, cells were stained with 0.5% (wt/vol) of Alcian Blue (in 3% (vol/vol) acetic acid) in 1:1 (culture:dye) ratio. This mixture was added to 10 μ L of 1% (wt/vol) low-melting point agarose beds (dissolved in BG11 medium) and covered with a coverslip. The preparations were observed using the light microscope Olympus DP25 Camera software Cell B.

Transcription Analysis by RT-qPCR

After extraction (for details see above), RNA concentration and purity (the ratios A₂₆₀/A₂₈₀ and A₂₆₀/A₂₃₀) were measured using a NanoDrop ND-1000 spectrophotometer (NanoDrop Technologies, Inc., United States). The quality and integrity of the RNA samples was also inspected in 1% (wt/vol) agarose gel performed by standard protocols using TAE buffer. The absence of genomic DNA contamination was checked by PCR, in reaction mixtures containing 0.5 U of GoTaq[®] G2 Flexi DNA Polymerase, 1x Green GoTaq Flexi buffer, 200 μ M of each dNTP, 1.5 mM MgCl₂, 0.25 μ M of each rnpB primer (Additional file 1: **Supplementary Table S4**), and 200 ng of total RNA. The PCR profile was: 5 min at 95°C followed by 25 cycles of 20 s at 95°C, 20 s at 56°C and 20 s at 72°C, and a final extension at 72°C for 5 min. The PCR reactions were run on 1% (wt/vol) agarose gel as described above. For cDNA synthesis, 1 μ g of total RNA was transcribed with the iScript[™] Reverse Transcription Supermix for RT-qPCR (Bio-Rad) in a final volume of 20 μ L, following the manufacturer's instructions. A control PCR was performed

using 1 μ L of cDNA as a template, the BD16S primers (Additional file 1: **Supplementary Table S4**), and the same reaction conditions and PCR program described above. Five-fold standard dilutions of the cDNAs were made (1/5, 1/25, 1/125, and 1/625) and stored at -20° C. RT-qPCRs were performed on Hard-Shell 384-Well PCR Plates (thin wall, skirted, clear/white) covered with Microseal[®] B adhesive seal (Bio-Rad). The reactions (10 μ L) were manually assembled and contained 0.125 μ M of each primer (Additional file 1: **Supplementary Table S4**), 5 μ L of iTaq[™] Universal SYBR[®] Green Supermix (Bio-Rad) and 1 μ L of template cDNA (dilution 1/5). The PCR protocol used was: 3 min at 95°C followed by 45 cycles of 30 s at 95°C, 30 s at 56°C, and 30 s at 72°C. In the end, a melting curve analysis of the amplicons (10 s cycles between 55 and 95°C with a 0.5°C increment per cycle) was conducted. Standard dilutions of the cDNA were used to check the relative efficiency and quality of primers, and negative controls (no template cDNA) included (for more details on RT-qPCR parameters see Additional file 1: **Supplementary Table S5**). RT-qPCRs were performed with three biological replicates and technical triplicates of each cDNA sample in the CFX384 Touch[™] Real-Time PCR Detection System (Bio-Rad). The data obtained were analyzed using the Bio-Rad CFX Maestro[™] 1.1 software, implementing an efficiency-corrected delta Cq method (Δ Cq). This method was used since the target genes *gsmt*, *dmt*, and *metX* were validated as reference genes using the reference gene selection tool available in the Maestro[™] software. For this reason, the relative expression of the targets is represented instead of the usual relative normalized expression. Statistical analysis was performed using a one-way ANOVA using the same software, and tests were considered significant if $p < 0.05$. The amplicon sizes were checked by agarose gel electrophoresis, and the DNA sequence was confirmed by Sanger sequencing. These experiments were compliant with the MIQE guidelines (Bustin et al., 2009), to promote the effort for experimental consistency and transparency, and to increase the reliability and integrity of the results obtained.

Compatible Solutes Quantification

Cultures of *Synechocystis* wild-type (WT), the Δ *sps*, Δ *ggpS*, and Δ *sps* Δ *ggpS* mutants and the strains harboring the GB device (WT, Δ *ggpS*, and Δ *sps* Δ *ggpS* backgrounds) were grown in BG11 or BG11 supplemented with 3% or 5% (wt/vol) NaCl, as described above, at an initial OD₇₃₀ \approx 0.5. The quantification of the CS—sucrose, glutamate, glucosylglycerol, and glycine betaine—was performed using 500 ml culture (distributed in 50 ml cultures in 100 ml Erlenmeyer flasks). Four days after inoculation, cells were harvested by centrifugation at 4,470 g for 10 min at room temperature (RT). In the case of the strains harboring the GB device, the extracellular medium was stored at -80° C, for further lyophilization and CS extraction. Cells were washed using 100 ml of cold distilled water, 3 or 5% (wt/vol) NaCl solutions (identical to the growth medium). Centrifugation was repeated and the cell pellets were resuspended in 50 ml of

the respective solutions. From this suspension, a 0.5 ml aliquot was centrifuged and stored at -20°C to be used later for protein quantification. The remaining cell suspension was centrifuged at 4°C and the cell pellet was stored at -20°C . Ethanol-chloroform extraction of the CS was performed as described in Ferreira et al. (2018) with adaptations. Briefly, cell pellets or lyophilized extracellular medium were suspended in 25 ml of 80% (vol/vol) ethanol and subsequently transferred to a 100 ml round flask containing a magnetic stir bar. The flask was connected to a coil condenser (circulating cold water) and heated at 100°C with stirring, for 10 min. The suspension was transferred to a 50 ml tube and centrifuged at 4,000 g for 10 min at RT. The supernatant was stored and the pellet resuspended in 20 ml of 80% (vol/vol) ethanol for a new extraction process. The remainder protocol was performed as described in Santos et al. (2006). Detection, identification and quantification of CS was performed by proton NMR. To that effect, freeze-dried extracts were dissolved in 1 ml of D_2O and a known amount of sodium formate was added to serve as an internal concentration standard. Spectra were acquired at 25°C on a Bruker Avance III 800 spectrometer (Bruker, Rheinstetten, Germany) working at a proton operating frequency of 800.33 MHz, equipped with a 5 mm, three channel, inverse detection cryoprobe TCI-z H&F/C/N with pulse-field gradients. A 3 s soft pulse was applied before the excitation pulse, to pre-saturate the water signal. Spectra were acquired under fully relaxed conditions (flip angle 60° ; repetition delay of 60 s) so that the area of the NMR signals was proportional to the amount of the different protons in the sample. Integration of the signals was performed using the tools available in the TopSpin software (Bruker, Rheinstetten, Germany) version 3.6.2. The concentration of CS was expressed as μmol per mg of protein. Protein extracts were obtained by sonication as described by Pinto et al. (2015), and protein quantification was performed using the Bio-Rad Protein Assay. For cell dry weight (DW) determinations, 40 ml of culture at $\text{OD}_{730} \approx 1.0$ (or equivalent) was centrifuged at 3,857 g for 10 min at RT. Then, the cell pellet was dried at 60°C for 48 h. Experiments included, at least, three biological replicates.

In silico Analysis of CS Production

The genome-scale metabolic model of *Synechocystis*—*iSyn811* (Montagud et al., 2011) –, was updated to include all the information required for the simulations. The manual curation process started with the addition of the final reaction in the synthesis of sucrose (“spp: $\text{H}_2\text{O} + \text{sucrose 6-phosphate} \rightarrow \text{phosphate} + \text{sucrose}$ ”), and also the metabolic precursors and the three reactions required for the synthesis of the heterologous CS, glycine betaine (“GSMT1: $S\text{-adenosyl-L-methionine} + \text{glycine} \leftrightarrow S\text{-adenosyl-L-homocysteine} + \text{sarcosine}$,” “GSMT2: $S\text{-adenosyl-L-methionine} + \text{sarcosine} \leftrightarrow S\text{-adenosyl-L-homocysteine} + N,N\text{-dimethylglycine}$,” and “DMT: $S\text{-adenosyl-L-methionine} + N,N\text{-dimethylglycine} \leftrightarrow S\text{-adenosyl-L-homocysteine} + N,N,N\text{-trimethylglycine}$ ”). In this process, the nomenclature was corrected and standardized (e.g., “glycerone” to “dihydroxy-acetone” or “GDP-mannose” to “GDP-D-mannose”), and the reversibility of some reactions changed (e.g., “sn-glycerol-

3-phosphate \rightarrow dihydroxy-acetone phosphate” to “sn-glycerol-3-phosphate \leftrightarrow dihydroxy-acetone phosphate”). Flux balance analysis (Orth et al., 2010) was performed to the *iSyn811* genome-scale metabolic reconstruction of *Synechocystis* for the production assessment of four different CS: three heterologous (glycine betaine, ectoine, and mannosylglycerate), and three native (glucosylglycerol, glutamate and sucrose). The MATLAB software, COBRA Toolbox v3.0 (Heirendt et al., 2019) was used for quantitative prediction of cellular and multicellular biochemical networks with constraint-based modelling. Simulations were constrained to match an autotrophic specific growth rate of 0.09/h, which corresponds to a light input of 0.8 mE/gDW/h and to a net carbon flux of 3.4 mmol/gDW/h into the cell, with CO_2 as carbon source. The description of the *iSyn811* model and further information on the simulation procedure are available in Montagud et al. (2010).

Statistical Analysis

The statistical analysis was performed by means of one- or two-way ANOVAs, using GraphPad Prism v6.01 (GraphPad Software Inc., United States).

RESULTS

Generation of *Synechocystis* Mutants Deficient in the Synthesis of Native Compatible Solutes

The sustainable production of heterologous compatible solutes using *Synechocystis* as a chassis was envisioned in this work. The starting step was the generation of mutants deficient in the production of one or both of the main native compatible solutes, sucrose, or glucosylglycerol (GG). For this purpose, the genes encoding the enzymes involved in the first step of sucrose or/and GG synthesis (*sps* and *ggpS*, respectively), were knocked out by double homologous recombination generating the *Synechocystis* markerless mutants Δsps , $\Delta ggpS$, and $\Delta sps\Delta ggpS$ (for details see *Materials*). The complete segregation of the mutants was confirmed by PCR and Southern blot (Additional file 1: **Supplementary Figures S1, S2**).

Effect of NaCl on the Growth of *Synechocystis* Wild-Type and the CS Deficient Mutants

The growth of the CS deficient mutants under different salinities was analyzed. *Synechocystis* WT and mutants Δsps , $\Delta ggpS$, and $\Delta sps\Delta ggpS$ were grown in standard BG11 medium or in BG11 supplemented with 3, 5, and 7% (wt/vol) NaCl, corresponding to 510, 860, and 1,200 mM, respectively. The growth was monitored by measuring the OD_{730} and chlorophyll *a* (chl *a*) content (**Figure 1**). In the absence of NaCl, the three mutants exhibited growth similar to the WT

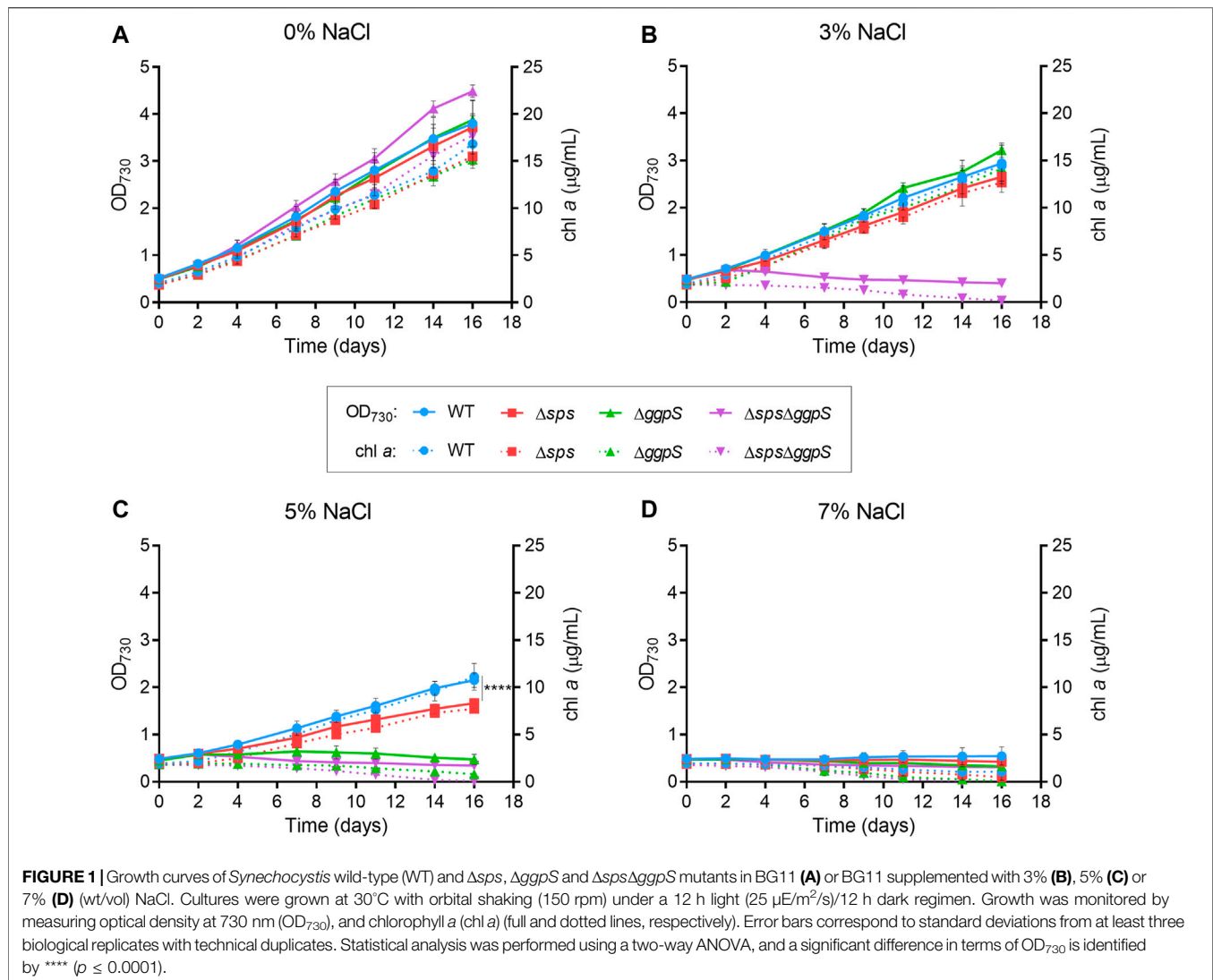


(Figure 1A), indicating that the synthesis of sucrose and/or GG is nonessential under standard growth conditions. Nonetheless, challenging the cells with 3% NaCl had clear detrimental effects, with a ~23% growth decrease observed for the WT and CS single mutants Δsps and $\Delta ggpS$ (Figure 1B; Additional file 1: Supplementary Table S1). The inactivation of both pathways in the $\Delta sps\Delta ggpS$ mutant led to total growth arrest accompanied by a decline in *chl a* content (Figure 1B; purple lines and Additional file 1: Supplementary Table S1). A more pronounced impact was observed by increasing NaCl to 5%. The $\Delta ggpS$ could not grow in these conditions, while for the WT and Δsps , a severe growth impairment (~49%) was observed (Figure 1C; Additional file 1: Supplementary Table S1). The growth of the latter two strains was similar up to day 7 however, after this period, the growth of Δsps slowed down and by day 16 there was a significant difference ($p \leq 0.0001$) compared with the WT. The *chl a* content confirmed these observations (Figure 1C; red and blue lines). Further increase in the NaCl concentration to 7% (wt/vol) showed that none of

the strains tested could withstand the stress imposed (Figure 1D; Additional file 1: Supplementary Table S1).

Quantification of CS in *Synechocystis* Wild-Type and the CS Deficient Mutants

The CS content was quantified in *Synechocystis* WT, Δsps , $\Delta ggpS$, and $\Delta sps\Delta ggpS$ mutants grown in BG11 or BG11 supplemented with NaCl (Figure 2), under salinity conditions in which each strain could sustain growth (Figure 1). In the WT, CS accumulation increased significantly in a salinity-dependent manner and GG was accumulated in higher amounts followed by glutamate and sucrose (Figure 2A). As expected, the two main compatible solutes sucrose and GG could only be detected in the presence of NaCl. The amino acid glutamate was detected in all backgrounds and conditions, and increased more than 1.8-fold in the presence of salinity (significant difference $p \leq 0.01$ for WT in 0 and 5% NaCl). In the Δsps , $\Delta ggpS$, and $\Delta sps\Delta ggpS$ mutants the absence of sucrose and/or GG production was confirmed

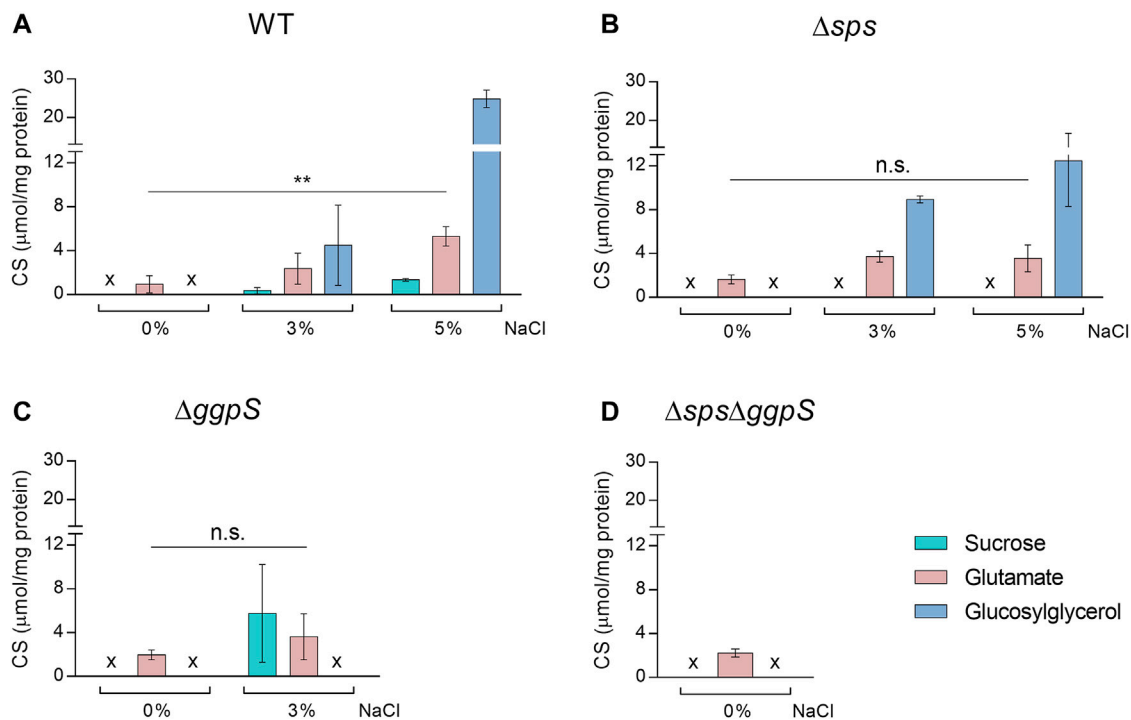


FIGURE 2 | Effect of NaCl on the synthesis of native compatible solutes sucrose, glutamate and glucosylglycerol by *Synechocystis* wild-type (WT) (A), and the Δsps (B), $\Delta ggpS$ (C), and $\Delta sps\Delta ggpS$ mutants (D). Cultures were grown in BG11 or BG11 supplemented with 3% or 5% (wt/vol) NaCl, at 30°C with orbital shaking (150 rpm) under a 12 h light (25 $\mu\text{E}/\text{m}^2/\text{s}$)/12 h dark regimen, and cells were harvested 4 days after inoculation (initial $\text{OD}_{730} \approx 0.5$). Compatible solutes were quantified by H-NMR and the results were normalized per mg of protein. x— not detected. Error bars correspond to standard deviations from at least three biological replicates. Statistical analysis was performed using two-way ANOVA. Statistically significant differences are identified: ** ($p \leq 0.01$) and n.s. (not significant).

(Figures 2B–D). For the Δsps , a salinity-dependent accumulation of GG was also detected (Figure 2B), however, the GG concentration was 50% lower compared with the WT, under 5% NaCl. In contrast, the $\Delta ggpS$ mutant accumulated 17-fold more sucrose than the WT, under 3% NaCl (Figure 2C). All the proton NMR spectra are depicted in Additional file 1: Supplementary Figure S3.

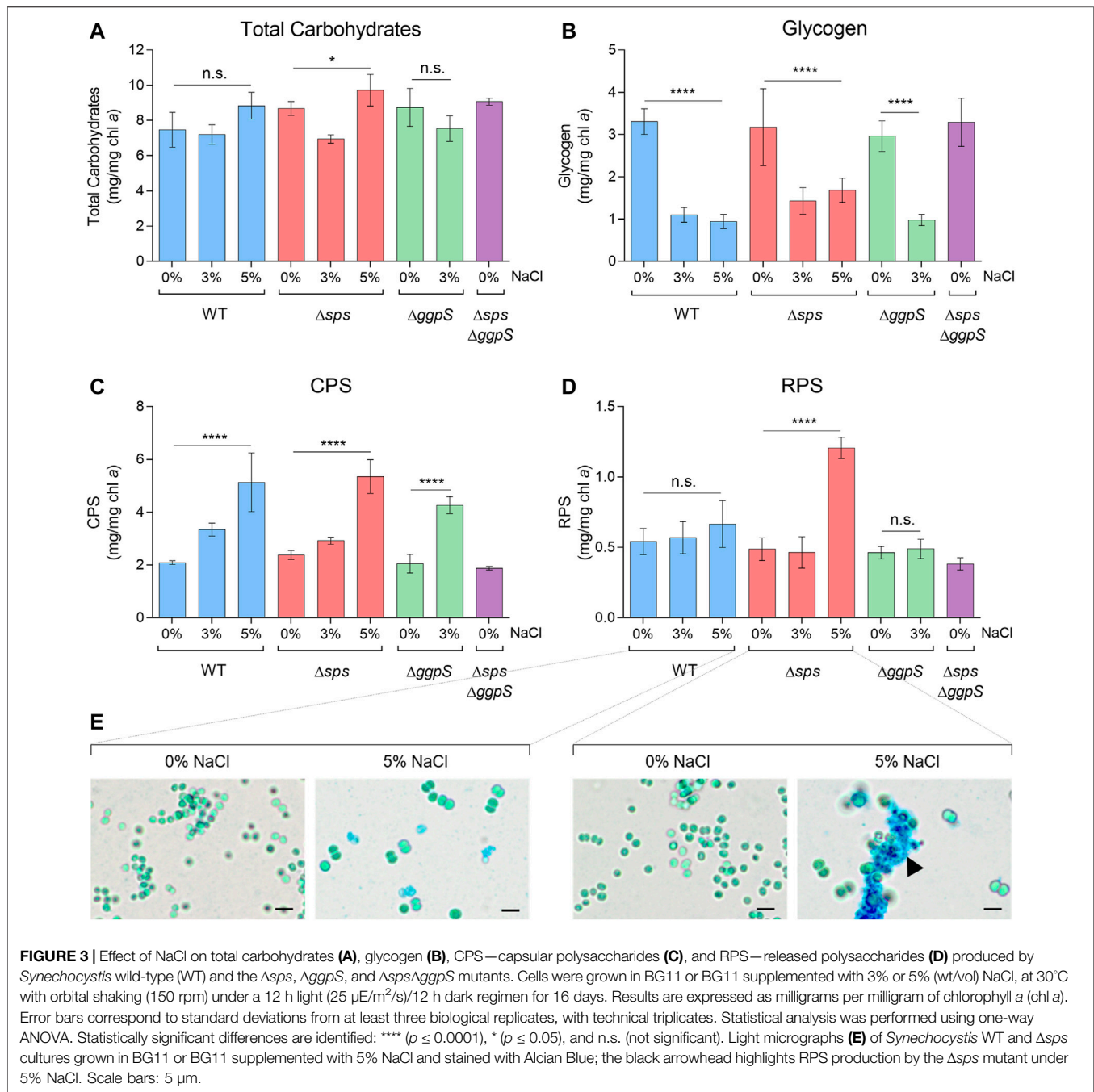
Effect of NaCl on Total Carbohydrates, Glycogen, Capsular, and Released Polysaccharides

In addition to the CS pools, the total carbohydrate content was analyzed in *Synechocystis* WT and the CS deficient mutants (Figure 3A). Generally, the presence of salinity (3 or 5% NaCl) had no significant impact on the production of total carbohydrates, except for the Δsps mutant that showed some fluctuation when exposed to different salinities (Figure 3A; $p \leq 0.05$). To further clarify the carbon distribution in response to salinity, the amount of glycogen as well as the production of extracellular polymeric substances, CPS and RPS, were also determined (Figures 3B–D). The presence of NaCl led to a significant decrease in the amount of glycogen in the WT, Δsps , and $\Delta ggpS$, with reductions of more than 56%, independent of the salinity concentration and the deletion of one of the CS pathways (Figure 3B). In terms of CPS, the opposite effect was observed with a 2.4-fold increase in CPS for the

WT and the Δsps at 5%, and a 2.1-fold increase for $\Delta ggpS$ at 3% NaCl, compared with 0% NaCl (Figure 3C). The amount of RPS produced by WT or $\Delta ggpS$ did not change significantly whereas for the Δsps a 2.5-fold increase was registered under 5% NaCl (Figure 3D). Staining the WT and Δsps cultures with Alcian Blue confirmed similar RPS production for the WT under 0 and 5% NaCl, while for the Δsps the accumulation of RPS in 5% NaCl is evident, leading to the formation of cell aggregates (Figure 3E; black arrowhead).

In silico Prediction of Production Rates for Native and Heterologous CS Using *Synechocystis* Wild-Type

The genome-scale metabolic model of *Synechocystis*—*iSyn811* (Montagud et al., 2011)—was updated to include all the information required for calculating CS production rates. The manual curation process started with the addition of the metabolic precursors and the reactions required for CS synthesis. The nomenclature was also corrected and standardized, and the reversibility of some reactions was changed (for more details see the Materials section). After the curation of the metabolic model was completed, the COBRA (“The COntstraint-Based Reconstruction and Analysis”) Toolbox v3.0 (Heirendt et al., 2019), was used to simulate the compatible solute production rate as a function of *Synechocystis* wild-type growth under autotrophic conditions (Figure 4). The results show a linear tradeoff between the cell’s



resources toward growth or the production of the different CS. Regarding the production of the native CS, GG, and sucrose impose a higher metabolic burden showing lower *in silico* production rates (0.378 and 0.283 mmol/gDW/h, respectively), compared with glutamate (0.567 mmol/gDW/h). The simulation of the production of heterologous CS glycine betaine (GB) showed the best compromise between growth and production compared with the three native CS, with the highest predicted maximum production rate of 0.680 mmol/gDW/h. In addition to GB, the production rates of other heterologous CS, such as ectoine and mannosylglycerate were also simulated, revealing that the

maximum production rate predicted for these two solutes is lower than the obtained for GB (Additional file 1: **Supplementary Figure S4**). Hence, GB was chosen as the heterologous CS to be produced using the *Synechocystis* chassis developed (CS-deficient mutants).

Design and Assembly of the Synthetic Device for the Production of Glycine Betaine

Envisaging the heterologous production of GB, a synthetic device was designed based on the metabolic pathway described for the

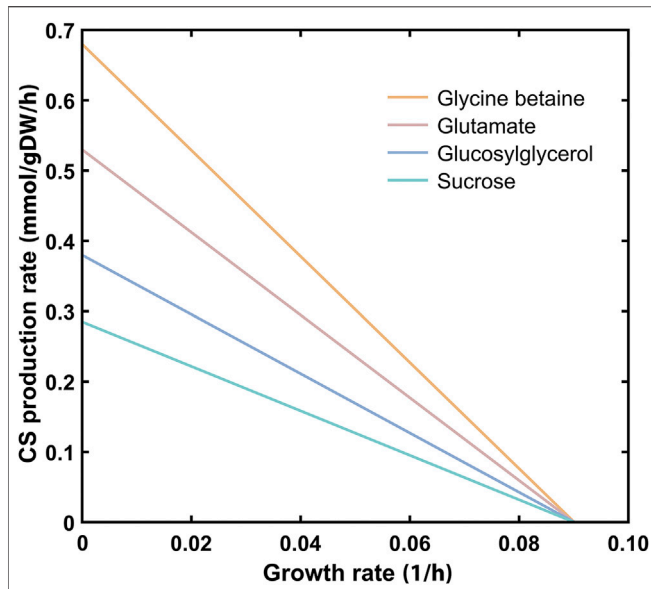


FIGURE 4 | Theoretical productivity of the heterologous compatible solute glycine betaine and the native ones (glutamate, glucosylglycerol, and sucrose), as predicted by the updated version of the genome-scale metabolic model *iSyn811*. The lines represent the compatible solute production rate as a function of *Synechocystis* wild-type growth under autotrophic conditions.

halophilic cyanobacterium *Aphanothece halophytica* (Figure 5A) (Nyyssola et al., 2000; Waditee et al., 2003). This device comprises two Open Reading Frames (ORFs) encoding the enzymes involved in the three-step methylation of glycine to glycine

betaine: glycine-sarcosine-*N*-methyltransferase (*gsmt*), and the dimethylglycine-*N*-methyltransferase (*dmt*). In these reactions, S-adenosylmethionine (SAM) is the source of methyl groups for the synthesis of GB, and it can be synthesized from L-methionine by the S-adenosyl-methionine synthase (MetX) (Figure 5A). To prevent the shortage of the SAM precursor, the ORF encoding *Synechocystis*' native MetX (*metX*, *sll0927*) was also included in the device. The sequences of the three ORFs (*gsmt*, *dmt*, and *metX*) were codon-optimized and restriction sites incompatible with the BioBrick standard RFC [10] were eliminated. Subsequently, the ribosome binding site (RBS) BBA_B0030 and double stop codons (TAATAA) were included before and after each ORF, respectively. A double terminator (BBA_B0015) was also included at the end of the synthetic construction (Ahbet). Additionally, the designed DNA sequence was flanked by the prefix and suffix of the BioBrick RFC [10] standard (Canton et al., 2008), enabling the use of the standard assembly method to include the regulatory element (promoter). After DNA synthesis, the Ahbet construction was cloned downstream of the promoter $P_{trc.x.lacO}$, originating the $P_{trc.x.lacO}::Ahbet$ synthetic device (hereafter GB device) (Figure 5B). The $P_{trc.x.lacO}$ is a constitutive promoter in *Synechocystis*, previously characterized by our group and is 41-fold stronger than the reference cyanobacterial promoter P_{rnpB} (Ferreira et al., 2018).

Effect of the Implementation of the GB Device Into the *Synechocystis* Chassis

The GB synthetic device was implemented into the *Synechocystis* WT and the CS deficient $\Delta ggpS$ and $\Delta sps\Delta ggpS$ chassis described above, using the replicative plasmid pSEVA351. The device was not introduced into

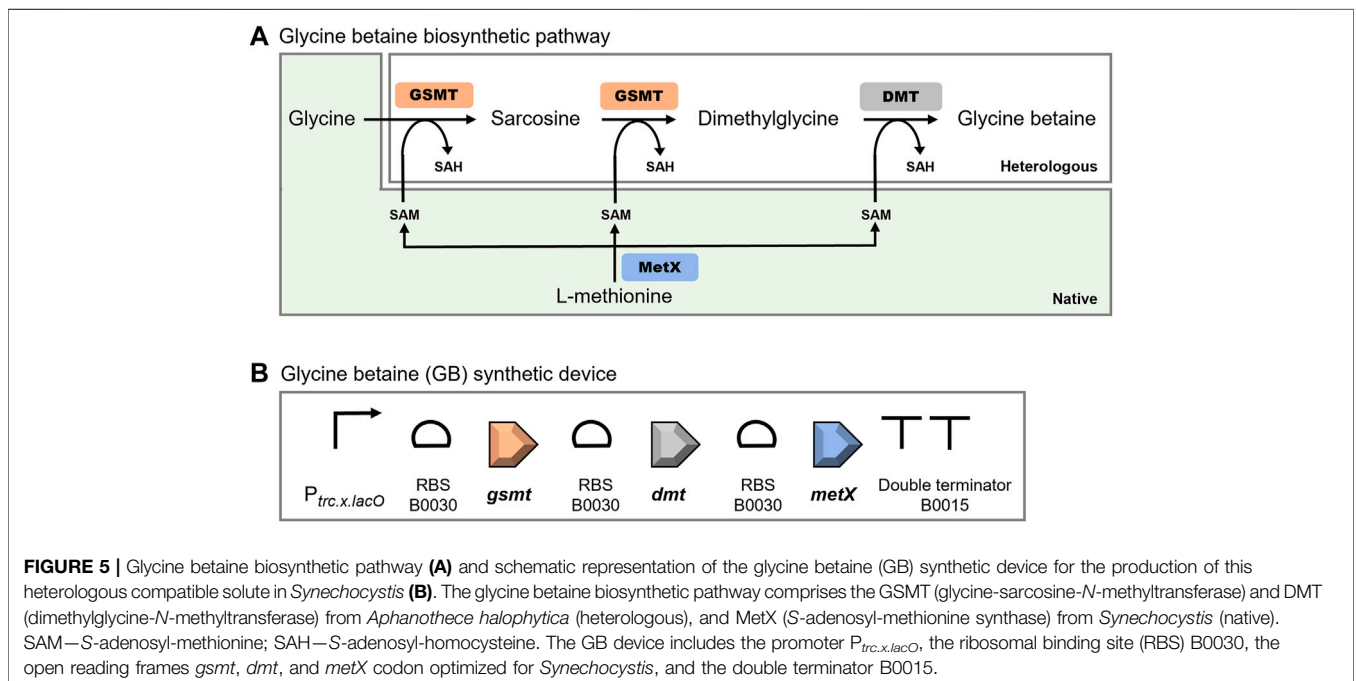


FIGURE 5 | Glycine betaine biosynthetic pathway (A) and schematic representation of the glycine betaine (GB) synthetic device for the production of this heterologous compatible solute in *Synechocystis* (B). The glycine betaine biosynthetic pathway comprises the GSMT (glycine-sarcosine-*N*-methyltransferase) and DMT (dimethylglycine-*N*-methyltransferase) from *Aphanothece halophytica* (heterologous), and MetX (S-adenosyl-methionine synthase) from *Synechocystis* (native). SAM—S-adenosyl-methionine; SAH—S-adenosyl-homocysteine. The GB device includes the promoter $P_{trc.x.lacO}$, the ribosomal binding site (RBS) B0030, the open reading frames *gsmt*, *dmt*, and *metX* codon optimized for *Synechocystis*, and the double terminator B0015.

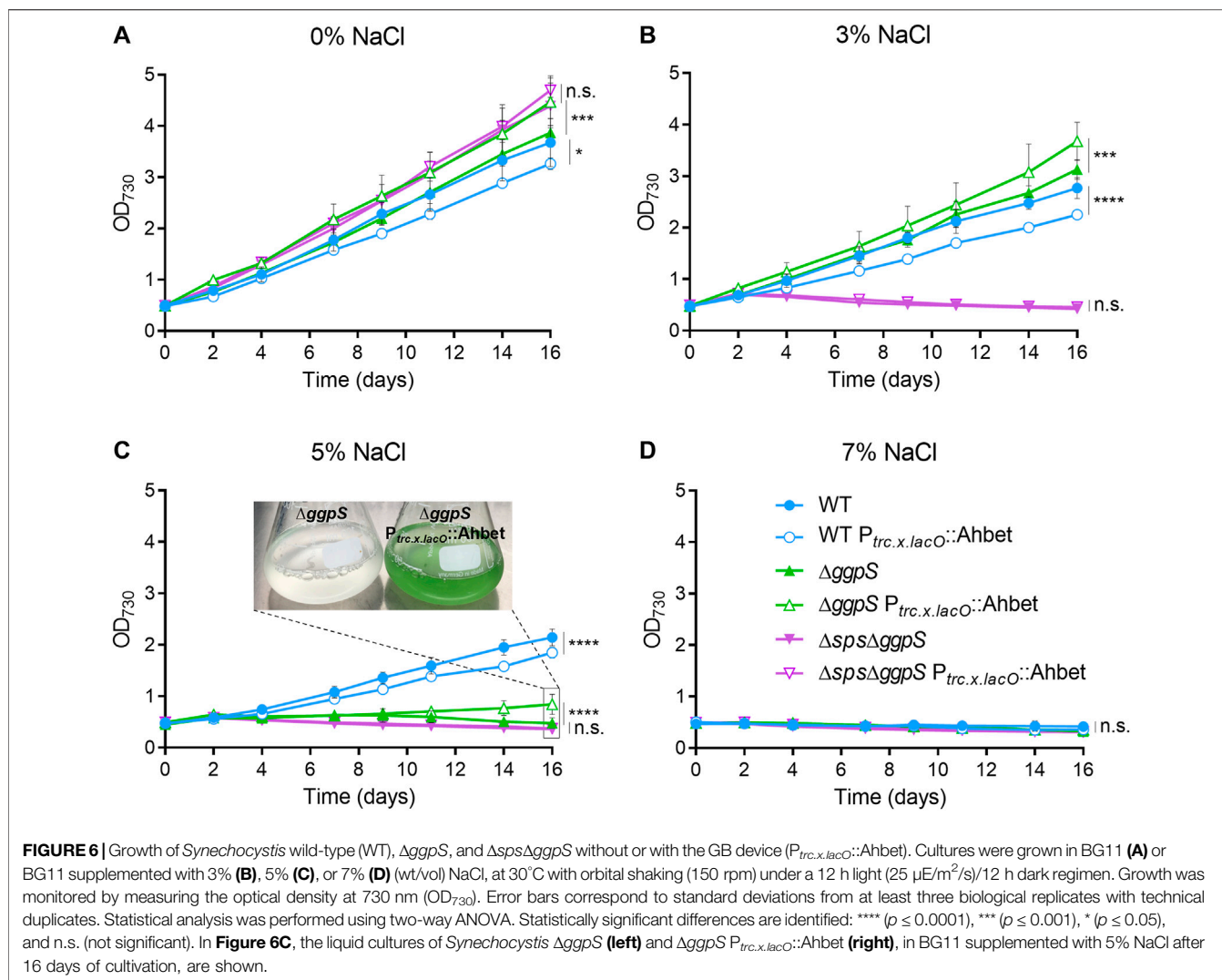


FIGURE 6 | Growth of *Synechocystis* wild-type (WT), Δ ggpS, and Δ sps Δ ggpS without or with the GB device (*P_{trc.x.lacO}::Ahbet*). Cultures were grown in BG11 (A) or BG11 supplemented with 3% (B), 5% (C), or 7% (D) (wt/vol) NaCl, at 30°C with orbital shaking (150 rpm) under a 12 h light (25 μ E/m²/s)/12 h dark regimen. Growth was monitored by measuring the optical density at 730 nm (OD₇₃₀). Error bars correspond to standard deviations from at least three biological replicates with technical duplicates. Statistical analysis was performed using two-way ANOVA. Statistically significant differences are identified: **** ($p \leq 0.0001$), *** ($p \leq 0.001$), * ($p \leq 0.05$), and n.s. (not significant). In **Figure 6C**, the liquid cultures of *Synechocystis* Δ ggpS (left) and Δ ggpS *P_{trc.x.lacO}::Ahbet* (right), in BG11 supplemented with 5% NaCl after 16 days of cultivation, are shown.

Δsps since the characterization showed that this mutant is similar to the WT in terms of growth, total carbohydrates, glycogen content and CPS (**Figure 1**, **Figures 3A–C**, respectively). The presence of the GB device in the cells was confirmed by PCR (Additional file 1: **Supplementary Figure S5**), and the growth and chl *a* content of the transformants were monitored in absence/presence of salinity and compared with the respective backgrounds (**Figure 6**; Additional file 1: **Supplementary Figure S6**). As shown in **Figure 6**, the introduction of the synthetic device had distinct effects depending on the genetic background. The implementation of GB device into Δ ggpS led to a significant improvement of growth (16%) in BG11 and BG11 supplemented with 3% NaCl (**Figures 6A,B**; green lines), and supported its survival under 5% NaCl (**Figure 6C**; green lines). After 16 days of cultivation under 5% NaCl, the batch culture of Δ ggpS showed clear signs of chlorosis/necrosis while the culture of the Δ ggpS mutant harboring the GB device remained green (**Figure 6C**;

insert). In agreement, the chl *a* content was 0.8 μ g/ml and 1.8 μ g/ml, respectively (Additional file 1: **Supplementary Figure S6**; green lines). Notably, this survival phenotype was observed for at least 25 days (data not shown). In the WT background the presence of the device had a detrimental effect on growth (~15% decrease) in all conditions tested (**Figure 6**; blue lines). The growth of the double mutant Δ sps Δ ggpS in the absence of NaCl was not affected by the introduction of the synthetic device (**Figure 6A**; purple lines). Moreover, the mutant harboring the GB device was unable to survive under saline conditions, similarly to what happened to Δ sps Δ ggpS background (**Figures 6B–D**; purple lines).

Analysis of Transcript Levels in *Synechocystis* Strains Harboring the GB Device

The next step in the characterization of the different *Synechocystis* strains harboring the GB device was the

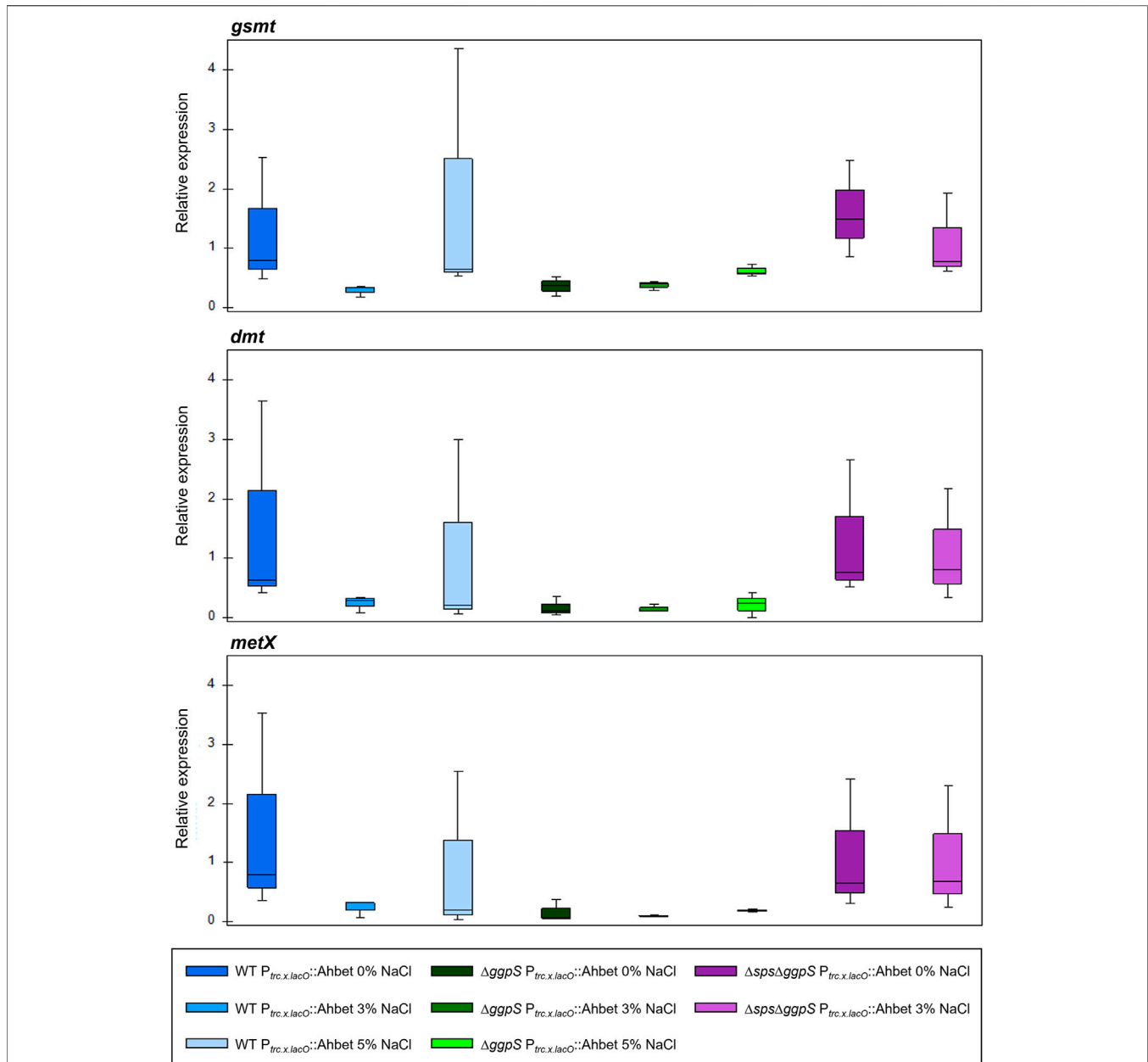


FIGURE 7 | RT-qPCR analysis of *gsmt*, *dmt*, and *metX* relative expression in *Synechocystis* strains (WT, $\Delta ggpS$, and $\Delta sps\Delta ggpS$) harboring the GB device. RNA was extracted from cells grown in BG11 or BG11 supplemented with 3 and 5% (wt/vol) NaCl, at 30°C with orbital shaking (150 rpm) under a 12 h light (25 $\mu E/m^2/s$)/12 h dark regimen. The box-whisker plots represent the expression of the target genes relative to WT $P_{trc.x.lacO}::Ahbet$ in absence of salt (0% NaCl). Data were obtained from three biological replicates and three technical replicates, and the whiskers represent the minimum and maximum non-outlier values in the dataset. One-way ANOVA was performed no significant differences could be detected.

evaluation of the transcript levels of the three ORFs comprised in the device (*gsmt*, *dmt*, and *metX*) by RT-qPCR (for more details see the *Materials* section). As shown in **Figure 7**, the transcripts of the three genes (*gsmt*, *dmt*, and *metX*) were detected in all samples and the relative expression was reasonably stable independently of the background strain. Additionally, the relative expression remained similar under salinity conditions and, even though some variation could be

detected, it was not statistically significant (Additional file 1: **Supplementary Table S2**).

Quantification of Native and Heterologous CS in *Synechocystis* Chassis Harboring the GB Device

The CS pool of the different *Synechocystis* strains (WT, $\Delta ggpS$, and $\Delta sps\Delta ggpS$) harboring the GB device was analyzed in

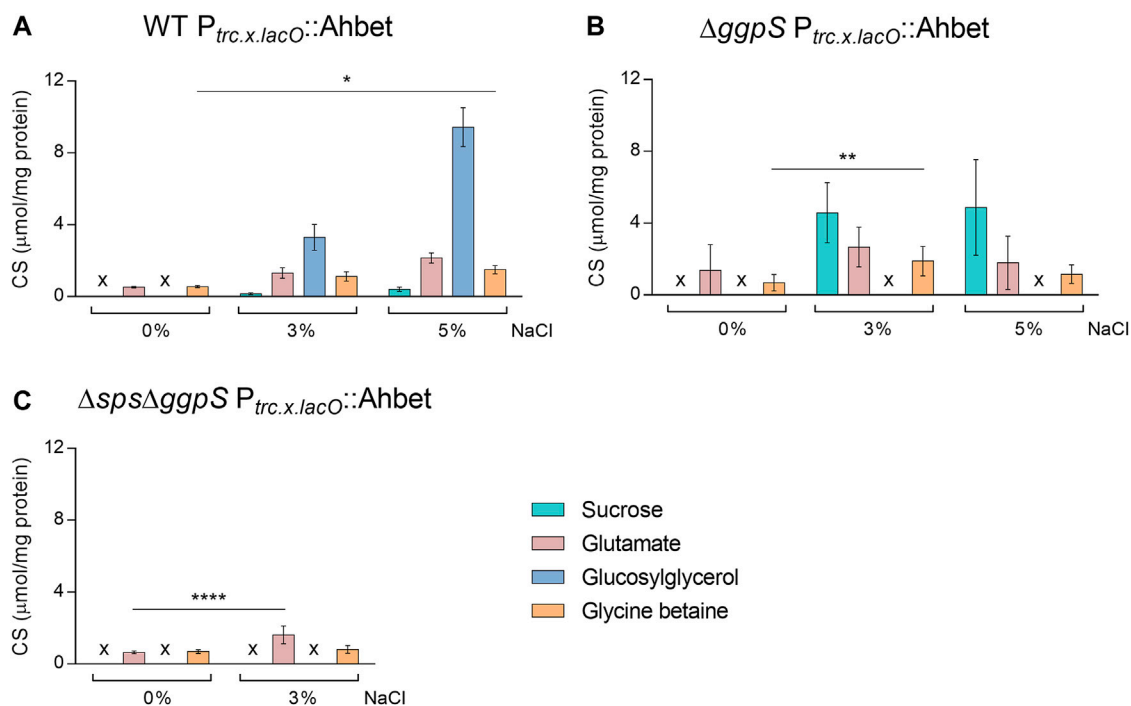


FIGURE 8 | Production of glycine betaine (GB) and native compatible solutes in different *Synechocystis* strains harboring the GB device: WT (wild-type) $P_{trc.x.lacO}::Ahbet$ (A), $\Delta ggpS P_{trc.x.lacO}::Ahbet$ (B), and $\Delta sps\Delta ggpS P_{trc.x.lacO}::Ahbet$ (C). Cultures were grown in BG11 or BG11 supplemented with 3% or 5% (wt/vol) NaCl, at 30°C with orbital shaking (150 rpm) under a 12 h light (25 $\mu E/m^2/s$)/12 h dark regimen; and cells were harvested 4 days after inoculation (initial $OD_{730} \approx 0.5$). Compatible solutes were quantified by H-NMR and the results were normalized per mg of protein. x— not detected. Error bars correspond to standard deviations from three biological replicates. Statistical analysis was performed using two-way ANOVA. Statistically significant differences are identified: **** ($p \leq 0.0001$), ** ($p \leq 0.01$), and * ($p \leq 0.05$).

absence/presence of NaCl after 4 days of cultivation (Figure 8). The results obtained confirmed that the implementation of the pathway for the synthesis of heterologous CS was successful, since glycine betaine could be detected in all strains and conditions analyzed. Under 0 and 3% NaCl, the presence of the GB device in the WT background did not significantly influence the synthesis of native CS and heterologous production of GB is not significantly influenced by salinity. However, under 5% NaCl, there was an impact on the synthesis of glutamate and GG that decreased by 59 and 62%, respectively, and the synthesis of GB increased 2.7-fold compared with 0% NaCl (Figures 2A, 8A). Similarly, the implementation of the device in the $\Delta ggpS$ did not affect the production of the native CS under 0 and 3% NaCl compared with $\Delta ggpS$ chassis (Figures 2C, 8B). However, the introduction of the device into the $\Delta ggpS$ background allowed this strain to survive under 5% NaCl and, therefore the quantification of CS was also performed. The results obtained showed that in $\Delta ggpS P_{trc.x.lacO}::Ahbet$, besides glycine betaine production, the levels of sucrose and glutamate were similar to the ones observed for 3% NaCl (Figure 8B). An analysis of the $\Delta ggpS$ harboring the GB device after 16 days of cultivation suggested that the production of all CS is maintained for at least 2 weeks of cultivation (Additional file 1: Supplementary Figure S7). For the double mutant, the presence of the device led to a significant decrease (71%) of glutamate in the absence of salinity (Figures 2D, 8C). In contrast, under 3% NaCl, there was a 2.5-fold increase

in glutamate ($p \leq 0.0001$) compared with 0% NaCl, while the glycine betaine content remained similar (Figure 8C). All the proton NMR spectra are depicted in Additional file 1: Supplementary Figure S8. Furthermore, the CS quantification was also performed for the extracellular medium, and the results showed that none of the native CS could be detected, while GB was detected in negligible amounts in all strains harboring the device and conditions tested (Additional file 1: Supplementary Table S3).

DISCUSSION

The sustainable production of compatible solutes (CS) is essential for pharmaceutical and cosmetic industries. The current microbiological processes have a significant negative impact on the environment, which could be mitigated by the use of photoautotrophic chassis such as cyanobacteria. For the synthesis of heterologous CS in *Synechocystis*, the construction of customized chassis is required and our strategy was to eliminate competing or redundant pathways. Therefore, in this work we have generated three *Synechocystis* mutants deficient in the production of native compatible solutes (namely, sucrose, or/ and glucosylglycerol). These strains— Δsps , $\Delta ggpS$, and $\Delta sps\Delta ggpS$ —were characterized under different salinity concentrations, expanding the knowledge that will allow

further optimization of the chassis for the increased production of heterologous CS, such as glycine betaine (GB). In this context, an updated version of the genome-scale metabolic model of *Synechocystis*—*iSyn811* (Montagud et al., 2011)—was used to predict the production rates for native and heterologous CS using *Synechocystis* wild-type. The simulations show a linear tradeoff between deviating resources toward cellular growth or toward the production of the solutes. Since energy and carbon uptake are limited, any extra need of ATP or carbon molecules for compatible solute synthesis will impair cell growth. Whether carbon or light uptake is limiting the synthesis of each CS is difficult to predict, since alternative routes with different energetic efficiencies can be simultaneously active under different growth conditions. From the CS evaluated, the predictions indicate that the synthesis of native sucrose, and glucosylglycerol (GG) has a higher impact on cell growth than glutamate or the heterologous solute glycine betaine (GB) (Figure 4). The production of sucrose and GG require glucose that drains more cell resources than the reported for the synthesis of an amino acid (Kaleta et al., 2013), such as glutamate or glycine (the latter required for GB production). The results also suggest that the production of GB has a smaller restraining effect on growth than glutamate or other heterologous CS, like ectoine and mannosylglycerate (Additional file 1: Supplementary Figure S4).

In parallel, the evaluation of the CS levels of the wild-type and the mutants (Δsps , $\Delta ggpS$, and $\Delta sps\Delta ggpS$) confirmed the salt-induced accumulation of sucrose and GG, which is well documented in the literature [for reviews see e.g., Klähn and Hagemann (2011); Hagemann (2013); Kirsch et al. (2019)]. In contrast, glutamate could be detected in the absence and presence of NaCl (Figure 2). These results are in agreement with the reported accumulation of this amino acid in *Synechocystis* grown in artificial seawater medium (ASW; 340 mM NaCl), and in BG11 supplemented with 12 mM KCl (Iijima et al., 2015; Iijima et al., 2020).

Previous works have also reported a tradeoff between the pools of different compatible solutes and other carbon sinks, such as glycogen or extracellular polymeric substances (EPS) in cyanobacteria (Du et al., 2013; Baran et al., 2017; Kirsch et al., 2017). In our work, the total carbohydrate content of *Synechocystis* WT and CS-deficient mutants remained unchanged when cells were exposed to NaCl, whereas a significant decrease in glycogen was observed (Figure 3). Concomitantly, the accumulation of capsular polysaccharides (CPS) was observed in a salinity-dependent manner and for the strains tested. In line with these observations is the increase in the levels of proteins involved in glycogen degradation, reported when *Synechocystis* cells were grown in ASW medium (Iijima et al., 2015). The protective role of EPS against salt stress was also demonstrated in a *Synechocystis* $\Delta sll1581\Delta slr1875$ double mutant, showing that a decrease in CPS content increases NaCl sensitivity (Jittawuttipoka et al., 2013). Altogether, these results strongly suggest that under saline conditions, *Synechocystis* breaks down glycogen and redirects carbon fluxes toward the production of CS and extracellular polysaccharides, promoting cell homeostasis and contributing to cell protection.

From the three *Synechocystis* CS-deficient mutants generated in this work, the Δsps was the only one able to grow in 5% NaCl. We also observed that this mutant's growth gets impaired over time, suggesting that the presence of sucrose is of additional importance for long-term cultivation. Accordingly, a previous work showed that Δsps cells in stationary phase were unable to survive a salt shock, which was not observed for cells in exponential phase; this effect could be prevented by sucrose supplementation (Desplats et al., 2005). Moreover, we show that the absence of sucrose leads to a severe reduction in the accumulation of GG whereas the released polysaccharides (RPS) increase significantly (1.8-fold), implying that extracellular polysaccharides production is crucial for the survival of the Δsps mutant under 5% NaCl. These results also suggest that sucrose role might go beyond osmoprotection, being involved in the regulation of metabolic pathways, e.g., triggering signaling cascades, as it was previously hypothesized by Desplats et al. (2005). For the $\Delta ggpS$ mutant an increased sucrose level was detected under 3% NaCl, showing that this sugar can sustain *Synechocystis*' survival under sea salt conditions for at least 16 days. Previously (Miao et al., 2003), generated a *Synechocystis* Δagp mutant unable to synthesize ADP-glucose (a precursor required for GG synthesis) that was also shown to accumulate high levels of sucrose and could survive upon a salt shock of 900 mM (5.2% NaCl). Notably, in the latter work and here, the mutant's sucrose levels were similar to GG accumulated in the WT cultivated under the same conditions. Taken together, these studies imply that GG and sucrose can have comparable osmoprotectant capacity when accumulated in similar levels. Additionally, the $\Delta sps\Delta ggpS$ mutant was unable to survive in any salt concentration tested and glutamate was the only CS that could be detected. Thus, this amino acid seems to have a minor contribution to the salt acclimation process in *Synechocystis*, similar to what was reported for the halophilic bacterium *Salinibacter ruber* (Oren et al., 2002).

Considering the metabolic model simulation, a synthetic device for the production of glycine betaine (GB) was designed and implemented into the *Synechocystis* wild-type and our customized chassis (CS-deficient mutants). Besides the ORFs required for GB production (*gsmt* and *dmt*) and *metX* (to prevent SAM shortage), this device comprises well-characterized regulatory elements: the synthetic promoter $P_{trc.xlacO}$ (Ferreira et al., 2018), the RBS BBa_B0030, and the double terminator BBa_B0015. This design ensured the stable constitutive transcription observed for the GB device ORFs, regardless of the chassis or salinity conditions (Figure 7), reinforcing that the use of orthogonal regulatory components is crucial to ensure the proper insulation of synthetic devices from the regulatory network of the chassis (Costello and Badran, 2021). Unlike transcription, the synthesis of the solute was not independent of cultivation conditions, and GB levels increased with salinity. In agreement, higher levels of glycine have been reported for *Synechocystis* cells grown in ASW medium compared with those grown in BG11 (Iijima et al., 2015). Since this amino acid is a precursor of GB, the high levels of glycine under salinity conditions most probably favor the synthesis of GB. In addition, glycogen degradation and carbon fluxes redirection

TABLE 2 | Native and heterologous production of glycine betaine via the three-step glycine methylation pathway.

| Native production | | | | | |
|--------------------------------------|---------------------------------------|--|--|-----------------------------------|----------------------------------|
| Strain | Salinity (mM) | Production capacity | Cultivation time | Reference | |
| <i>Aphanothece halophytica</i> | 2,000 | 0.06 $\mu\text{mol}/\text{mg}$ protein | 1 h | Ishitani et al. (1993) | |
| <i>Aphanothece halophytica</i> | 2,000 | $\sim 0.4 \mu\text{mol}/10^7$ cells | 7 days | Incharoensakdi and Waditee (2000) | |
| <i>Aphanothece halophytica</i> | 1,500 | $\sim 40,000 \mu\text{mol}/\text{gFW}$ | 10 days | Waditee et al. (2007) | |
| <i>Aphanothece halophytica</i> | 2,000 | 20.1 $\mu\text{mol}/\text{gFW}$ | 15 days | Waditee-Sirisattha et al. (2015) | |
| Heterologous production | | | | | |
| Production strain | Native strain | Salinity (mM) | Production capacity | Cultivation time | Reference |
| <i>Arabidopsis thaliana</i> | <i>Aphanothece halophytica</i> | 100 | $\sim 2 \mu\text{mol}/\text{gFW}$ | 15 days | Waditee et al. (2005) |
| <i>Nicotiana tabacum</i> | <i>Aphanothece halophytica</i> | 0 | 0.4 $\mu\text{mol}/\text{gFW}$ | 28 days | He et al. (2011) |
| <i>Synechococcus</i> PCC 7942 | <i>Aphanothece halophytica</i> | 500 | $\sim 1.5 \mu\text{mol}/\text{gFW}$ | NA | Waditee et al. (2005) |
| <i>Anabaena</i> sp. PCC 7120 | <i>Aphanothece halophytica</i> | 140 | 0.04 $\mu\text{mol}/\text{gFW}$ | 7 days | Waditee-Sirisattha et al. (2012) |
| <i>Anabaena doliolum</i> | <i>Aphanothece halophytica</i> | 500 | 12.92 $\mu\text{mol}/\text{gDW}$ | 10 days | Singh et al. (2013) |
| <i>Synechocystis</i> sp. PCC 6803 | <i>Aphanothece halophytica</i> | 510 | 64.29 $\mu\text{mol}/\text{gDW}$ | 4 days | This work |
| <i>Escherichia coli</i> XL1-Blue | <i>Ectothiorhodospira halochloris</i> | 300 | 78 $\mu\text{mol}/\text{gDW}$ | NA | Nyysola et al. (2000) |
| <i>Escherichia coli</i> BL21 | <i>Aphanothece halophytica</i> | 300 | $\sim 23 \mu\text{mol}/\text{gDW}$ | 3 h | Waditee et al. (2003) |
| <i>Escherichia coli</i> BL21 | <i>Aphanothece halophytica</i> | 300 | $\sim 2,000 \mu\text{mol}/\text{mg}$ protein | 3 h | Waditee et al. (2007) |
| <i>Escherichia coli</i> BL21 | <i>Aphanothece halophytica</i> | 300 | $\sim 80 \mu\text{mol}/\text{L}$ | 2 h | He et al. (2011) |
| <i>Escherichia coli</i> DH5 α | <i>Aphanothece halophytica</i> | 500 | 6 $\mu\text{mol}/\text{gDW}$ | 24 h | Waditee-Sirisattha et al. (2012) |
| <i>Escherichia coli</i> DH5 α | <i>Aphanothece halophytica</i> | 0 | 80.62 $\mu\text{mol}/\text{gDW}$ | ON | Singh et al. (2013) |
| <i>Pseudomonas denitrificans</i> | <i>Aphanothece halophytica</i> | 0 | NA* | 1 day | Shkryl et al. (2020) |

ON, overnight; NA, not available; DW, dry weight; FW, fresh weight; *—Identified by HPLC-MS.

toward the production of CS could also explain the increased amount of GB produced in the presence of NaCl.

The implementation of the GB device into *Synechocystis* wild-type led to a small decrease in growth in all conditions tested (Figure 6). As predicted by the metabolic flux model, the device may drain the cell's resources imposing a metabolic burden, causing growth impairment. This can be explained by the redirection of part of the photosynthetically fixed carbon to the synthesis of CS, which is no longer available for biomass formation, similarly to what was reported for the production of mannitol (Wu et al., 2020). In contrast to what was observed for the WT, the introduction of the GB device into the ΔggpS mutant resulted in an increased salt tolerance with the concomitant growth improvement, enabling its survival under 5% NaCl. This phenotype was maintained under long-term cultivation periods up to 25 days (data not shown), suggesting that GB can compensate for the absence of GG. Conversely, the implementation of the GB device in the $\Delta\text{sps}\Delta\text{ggpS}$ mutant did not improve its performance under salinity conditions. However, it remains unclear if this outcome is due to: 1) insufficient production of glycine betaine to allow cell survival or 2) the absence of both native compatible solutes (sucrose and GG).

In terms of production, the highest GB amount was obtained for the ΔggpS cultivated in BG11 supplemented with 3% NaCl for 4 days (1.89 μmol GB/mg protein, corresponding to 64.29 $\mu\text{mol}/\text{gDW}$, and a volumetric productivity of 13.67 $\mu\text{g}/\text{L}/\text{h}$) (Figure 8B). Unexpectedly, the production of GB was not higher at 5% NaCl, which may be due to the limited capacity of the cells to survive in such conditions. Extending the cultivation period up to 16 days does not seem to affect the

synthesis of GB in any condition tested (Supplementary Figure S7), suggesting that the process is stable. In addition, the negligible GB amounts detected in the extracellular medium show that this CS can be exported. Since product secretion facilitates recovery and reduces costs, this aspect should be addressed in the establishment of a GB-cell factory.

The production of GB using native organisms and heterologous hosts (with the synthesis of the solute mainly based on the metabolic pathway described for *A. halophytica*), has been previously reported (Table 2). However, a direct comparison is difficult since different normalization methods were used, and the cultivation conditions/time periods need also to be taken into consideration. Generally, the use of native GB producers such as the hypersaline cyanobacterium *A. halophytica* can render high amounts of the solute. This entails major disadvantages related to the high salt concentrations required, such as the reduced durability of the bioreactors, long processes, and detrimental impact on the environment. In contrast, with heterologous hosts the salinity concentrations used are at least 1/3 of those employed for *A. halophytica* (Table 2—heterologous production). Considering the photoautotrophic organisms, the amounts obtained using plants are low and require rather long cultivation periods. The most promising results were obtained using the filamentous cyanobacterium *Anabaena doliolum* that produced 12.92 μmol GB/gDW after 10 days of cultivation (Singh et al., 2013). Using our *Synechocystis* ΔggpS chassis, we report a production level ~ 5 -fold higher than that of *A. doliolum* in just 4 days of cultivation (64.29 μmol GB/gDW). Regarding the heterotrophic chassis, the GB amounts obtained using different *Escherichia coli* strains were only up to 1.25-fold higher than with *Synechocystis* ΔggpS . Cultivation times are significantly reduced for heterotrophic bacteria, but the use of photoautotrophic

chassis enables CO₂ fixation promoting bio-mitigation and surpassing the need to supply a carbon source. Additionally, the highest GB production by our *Synechocystis* Δ ggpS chassis was achieved under 510 mM NaCl, opening up the possibility of large-scale cultivation with seawater (salinity range 3.1–3.8%). This does not seem as viable with *E. coli* since increasing the salt concentration to 500 mM has a substantial detrimental impact on the GB production (Waditee-Sirisattha et al., 2012).

CONCLUSION

The heterologous production of the compatible solute glycine betaine (GB) was successfully achieved in different *Synechocystis*-based chassis. The characterization of these compatible solutes (CS) deficient chassis (Δ sps, Δ ggpS, and Δ sps Δ ggpS) revealed that under saline conditions, the carbon fluxes are redirected from the synthesis of glycogen toward the production of CS and extracellular polysaccharides. In fact, the maximum amount of GB was obtained in Δ ggpS harboring the GB device, under 3% NaCl (64.29 μ mol/gDW). This production level is promising and not far from applications using *E. coli*. Considering that the knowledge generated by the characterization of the CS deficient mutants will allow the identification of potential targets to optimize our chassis, that our GB production is based on sunlight and CO₂ fixation, and that there is the possibility of using seawater, *Synechocystis* emerges as a feasible photoautotrophic chassis for large-scale heterologous production of GB or other CS.

DATA AVAILABILITY STATEMENT

The original contributions presented in the study are included in the article/**Supplementary Material**, further inquiries can be directed to the corresponding author.

AUTHOR CONTRIBUTIONS

CCP, EAF, FP, and PT were involved in the conceptual design of the work. The experimental design and strain engineering were carried out by EAF, CCP, JSR, and FP. Characterization and data analysis were performed by EAF and CCP. CS quantification by

proton NMR was carried out by PL. EAF, DF, and JU were involved in the curation, simulations, and analyses involving the *iSyn* metabolic model. Data interpretation and article preparation was performed by EAF, CCP, DF (*iSyn* metabolic model), and PT. All authors have revised and approved the submitted version of the article.

FUNDING

This work was financed by Portuguese funds through the Fundação para a Ciência e a Tecnologia (FCT)/Ministério da Ciência, Tecnologia e Ensino Superior within the scope of UIDB/04293/2020, and UIDP/04293/2020. We also greatly acknowledge FCT for the scholarship SFRH/BD/117508/2016 (EAF) and the Assistant Researcher contracts CEECIND/00259/2017 (CCP) and 2020.01953.CEECIND (FP). The NMR data were acquired at CERMAX, ITQB-NOVA, Oeiras, Portugal with equipment funded by FCT, project AAC 01/SAICT/2016.

ACKNOWLEDGMENTS

The authors acknowledge the technical and scientific support of the i3S Scientific Platform “Cell Culture and Genotyping” in the RT-qPCR experiments. We are grateful to: Prof. Paula Gomes, Dr. Luísa Aguiar, and Mélanie Fonte (LAQV-REQUIMTE, Faculdade de Ciências, Universidade do Porto) for providing the equipment and technical assistance regarding compatible solutes extraction; Dr. Paulo Oliveira (i3S) for all the support provided, the scientific discussions, and suggestions; and Dr. Maria Siurana (UPV) for the scientific discussions regarding the *iSyn* metabolic model. The content of this article is available as a preprint at: <https://doi.org/10.21203/rs.3.rs-1031622/v1> (Ferreira et al., 2021).

SUPPLEMENTARY MATERIAL

The Supplementary Material for this article can be found online at: <https://www.frontiersin.org/articles/10.3389/fbioe.2021.821075/full#supplementary-material>

REFERENCES

- Ananya, A. K., and Ahmad, I. Z. (2014). Cyanobacteria" the Blue green Algae" and its Novel Applications: A Brief Review. *IJIAS* 7, 251–261.
- Baran, R., Lau, R., Bowen, B. P., Diamond, S., Jose, N., Garcia-Pichel, F., et al. (2017). Extensive Turnover of Compatible Solutes in Cyanobacteria Revealed by Deuterium Oxide (D₂O) Stable Isotope Probing. *ACS Chem. Biol.* 12, 674–681. doi:10.1021/acschembio.6b00890
- Bustin, S. A., Benes, V., Garson, J. A., Hellemans, J., Huggett, J., Kubista, M., et al. (2009). The MIQE Guidelines: Minimum Information for Publication of Quantitative Real-Time PCR Experiments. *Clin. Chem.* 55, 611–622. doi:10.1373/clinchem.2008.112797
- Caldas, T., Demont-Caulet, N., Ghazi, A., and Richarme, G. (1999). Thermoprotection by glycine Betaine and Choline. *Microbiol* 145, 2543–2548. doi:10.1099/00221287-145-9-2543
- Canton, B., Labno, A., and Endy, D. (2008). Refinement and Standardization of Synthetic Biological Parts and Devices. *Nat. Biotechnol.* 26, 787–793. doi:10.1038/nbt1413
- Cholewa, J. M., Guimarães-Ferreira, L., and Zanchi, N. E. (2014). Effects of Betaine on Performance and Body Composition: a Review of Recent Findings and Potential Mechanisms. *Amino Acids* 46, 1785–1793. doi:10.1007/s00726-014-1748-5
- Cleland, D., Krader, P., McCree, C., Tang, J., and Emerson, D. (2004). Glycine Betaine as a Cryoprotectant for Prokaryotes. *J. Microbiol. Methods* 58, 31–38. doi:10.1016/j.mimet.2004.02.015

- Costello, A., and Badran, A. H. (2021). Synthetic Biological Circuits within an Orthogonal Central Dogma. *Trends Biotechnol.* 39, 59–71. doi:10.1016/j.tibtech.2020.05.013
- Day, C. R., and Kempson, S. A. (2016). Betaine Chemistry, Roles, and Potential Use in Liver Disease. *Biochim. Biophys. Acta (BBA) - Gen. Subjects* 1860, 1098–1106. doi:10.1016/j.bbagen.2016.02.001
- Desplats, P., Folco, E., and Salerno, G. L. (2005). Sucrose May Play an Additional Role to that of an Osmolyte in *Synechocystis* sp. PCC 6803 Salt-Shocked Cells. *Plant Physiol. Biochem.* 43, 133–138. doi:10.1016/j.plaphy.2005.01.008
- Dikilitas, M., Simsek, E., and Roychoudhury, A. (2020). “Role of Proline and glycine Betaine in Overcoming Abiotic Stresses,” in *Protective Chemical Agents in the Amelioration of Plant Abiotic Stress: Biochemical and Molecular Perspectives*. Editors A. Roychoudhury and D. K. Tripathi (John Wiley & Sons), 1–23. doi:10.1002/9781119552154.ch1
- Du, W., Liang, F., Duan, Y., Tan, X., and Lu, X. (2013). Exploring the Photosynthetic Production Capacity of Sucrose by Cyanobacteria. *Metab. Eng.* 19, 17–25. doi:10.1016/j.ymben.2013.05.001
- Dubois, M., Gilles, K. A., Hamilton, J. K., Rebers, P. A., and Smith, F. (1956). Colorimetric Method for Determination of Sugars and Related Substances. *Anal. Chem.* 28, 350–356. doi:10.1021/ac60111a017
- DuPont (2015). Betafin® Natural Betaine Sustainable and Substantiated. Available at: http://animalnutrition.dupont.com/fileadmin/user_upload/live/animal_nutrition/documents/open/Betafin__Natural_Betaine_Lifecycle_Analysis.pdf (Accessed October 14, 2021).
- Eklund, M., Bauer, E., Wamatu, J., and Mosenthin, R. (2005). Potential Nutritional and Physiological Functions of Betaine in Livestock. *Nutr. Res. Rev.* 18, 31–48. doi:10.1079/nrr200493
- Ernst, A., Kirschenlohr, H., Diez, J., and Böger, P. (1984). Glycogen Content and Nitrogenase Activity in *Anabaena Variabilis*. *Arch. Microbiol.* 140, 120–125. doi:10.1007/bf00454913
- Ferreira, E. A., Pacheco, C. C., Pinto, F., Pereira, J., Lamosa, P., Oliveira, P., et al. (2018). Expanding the Toolbox for *Synechocystis* sp. PCC 6803: Validation of Replicative Vectors and Characterization of a Novel Set of Promoters. *Synth. Biol. (Oxf)* 3, ysy014. doi:10.1093/synbio/ysy014
- Ferreira, E. A., Pacheco, C. C., Rodrigues, J. S., Pinto, F., Lamosa, P., Fuente, D., et al. (2021). Heterologous Production of glycine Betaine Using *Synechocystis* sp. PCC 6803-based Chassis Lacking Native Compatible Solutes, Preprint. *Res. Square* (Accessed November 22, 2021). doi:10.21203/rs.3.rs-1031622/v1
- Gopalakrishnan, S., Pakrasi, H. B., and Maranas, C. D. (2018). Elucidation of Photoautotrophic Carbon Flux Topology in *Synechocystis* PCC 6803 Using Genome-Scale Carbon Mapping Models. *Metab. Eng.* 47, 190–199. doi:10.1016/j.ymben.2018.03.008
- Grossman, E. B., and Hebert, S. C. (1989). Renal Inner Medullary Choline Dehydrogenase Activity: Characterization and Modulation. *Am. J. Physiology-Renal Physiol.* 256, F107–F112. doi:10.1152/ajprenal.1989.256.1.f107
- Guinn, E. J., Pegram, L. M., Capp, M. W., Pollock, M. N., and Record, M. T. (2011). Quantifying Why Urea Is a Protein Denaturant, whereas glycine Betaine Is a Protein Stabilizer. *Proc. Natl. Acad. Sci.* 108, 16932–16937. doi:10.1073/pnas.1109372108
- Hagemann, M. (2013). “Genomics of Salt Acclimation,” in *Adv Bot Res.* Editor C. C.-C. Franck Chauvat (Academic Press), 65, 27–55. doi:10.1016/b978-0-12-394313-2.00002-0
- Hays, S. G., and Ducat, D. C. (2015). Engineering Cyanobacteria as Photosynthetic Feedstock Factories. *Photosynth Res.* 123, 285–295. doi:10.1007/s11120-014-9980-0
- He, Y., He, C., Li, L., Liu, Z., Yang, A., and Zhang, J. (2011). Heterologous Expression of *ApGSM2* and *ApDMT2* Genes from *Aphanothece Halophytica* Enhanced Drought Tolerance in Transgenic Tobacco. *Mol. Biol. Rep.* 38, 657–666. doi:10.1007/s11033-010-0152-9
- Heidorn, T., Camsund, D., Huang, H.-H., Lindberg, P., Oliveira, P., Stensjö, K., et al. (2011). “Synthetic Biology in Cyanobacteria,” in *Methods Enzymol.* Editor C. Voigt (Academic Press), 497, 539–579. doi:10.1016/b978-0-12-385075-1.00024-x
- Heikkilä, H. O., Melaja, J. A., Millner, D. E., and Virtanen, J. J. (1982). Betaine Recovery Process. US4359430A.
- Heirendt, L., Arreckx, S., Pfau, T., Mendoza, S. N., Richelle, A., Heinken, A., et al. (2019). Creation and Analysis of Biochemical Constraint-Based Models Using the COBRA Toolbox v.3.0. *Nat. Protoc.* 14, 639–702. doi:10.1038/s41596-018-0098-2
- Holmström, K. O., Somersalo, S., Mandal, A., Palva, T. E., and Welin, B. (2000). Improved Tolerance to Salinity and Low Temperature in Transgenic Tobacco Producing glycine Betaine. *J. Exp. Bot.* 51, 177–185. doi:10.1093/jexbot/51.343.177
- Huang, H.-H., Camsund, D., Lindblad, P., and Heidorn, T. (2010). Design and Characterization of Molecular Tools for a Synthetic Biology Approach towards Developing Cyanobacterial Biotechnology. *Nucleic Acids Res.* 38, 2577–2593. doi:10.1093/nar/gkq164
- Iijima, H., Nakaya, Y., Kuwahara, A., Hirai, M. Y., and Osanai, T. (2015). Seawater Cultivation of Freshwater Cyanobacterium *Synechocystis* sp. PCC 6803 Drastically Alters Amino Acid Composition and Glycogen Metabolism. *Front. Microbiol.* 6, 326. doi:10.3389/fmicb.2015.00326
- Iijima, H., Watanabe, A., Sukigara, H., Shirai, T., Kondo, A., and Osanai, T. (2020). Simultaneous Increases in the Levels of Compatible Solutes by Cost-effective Cultivation of *Synechocystis* sp. PCC 6803. *Biotechnol. Bioeng.* 117, 1649–1660. doi:10.1002/bit.27324
- Inchareonsakdi, A., and Waditee, R. (2000). Degradation of Glycinebetaine by Betaine-Homocysteine Methyltransferase in *Aphanothece halophytica*: Effect of Salt Downshock and Starvation. *Curr. Microbiol.* 41, 227–231. doi:10.1007/s002840010125
- Ishitani, M., Takabe, T., Kojima, K., and Takabe, T. (1993). Regulation of Glycinebetaine Accumulation in the Halotolerant Cyanobacterium *Aphanothece Halophytica*. *Funct. Plant Biol.* 20, 693–703. doi:10.1071/pp9930693
- Jittawuttipoka, T., Planchon, M., Spalla, O., Benzerara, K., Guyot, F., Cassier-Chauvat, C., et al. (2013). Multidisciplinary Evidences that *Synechocystis* PCC6803 Exopolysaccharides Operate in Cell Sedimentation and protection against Salt and Metal Stresses. *PLoS One* 8, e55564. doi:10.1371/journal.pone.0055564
- Joshi, C. J., Peebles, C. A. M., and Prasad, A. (2017). Modeling and Analysis of Flux Distribution and Bioproduct Formation in *Synechocystis* sp. PCC 6803 Using a New Genome-Scale Metabolic Reconstruction. *Algal Res.* 27, 295–310. doi:10.1016/j.algal.2017.09.013
- Kaletka, C., Schäuble, S., Rinas, U., and Schuster, S. (2013). Metabolic Costs of Amino Acid and Protein Production in *Escherichia coli*. *Biotechnol. J.* 8, 1105–1114. doi:10.1002/biot.201200267
- Kanesaki, Y., Shiwa, Y., Tajima, N., Suzuki, M., Watanabe, S., Sato, N., et al. (2012). Identification of Substrain-specific Mutations by Massively Parallel Whole-Genome Resequencing of *Synechocystis* sp. PCC 6803. *DNA Res.* 19, 67–79. doi:10.1093/dnares/dsr042
- Kar, J. R., Hallsworth, J. E., and Singhal, R. S. (2015). Fermentative Production of glycine Betaine and Trehalose from Acid Whey Using *Actinopolyspora Halophila* (MTCC 263). *Environ. Tech. Innovation* 3, 68–76. doi:10.1016/j.eti.2015.02.001
- Kirsch, F., Klähn, S., and Hagemann, M. (2019). Salt-regulated Accumulation of the Compatible Solutes Sucrose and Glucosylglycerol in Cyanobacteria and its Biotechnological Potential. *Front. Microbiol.* 10, 2139. doi:10.3389/fmicb.2019.02139
- Kirsch, F., Pade, N., Klähn, S., Hess, W. R., and Hagemann, M. (2017). The Glucosylglycerol-Degrading Enzyme GghA Is Involved in Acclimation to Fluctuating Salinities by the Cyanobacterium *Synechocystis* sp. Strain PCC 6803. *Microbiol* 163, 1319–1328. doi:10.1099/mic.0.000518
- Klähn, S., and Hagemann, M. (2011). Compatible Solute Biosynthesis in Cyanobacteria. *Environ. Microbiol.* 13, 551–562. doi:10.1111/j.1462-2920.2010.02366.x
- Knoll, A. H. (2008). “Cyanobacteria and Earth History,” in *The Cyanobacteria: Molecular Biology, Genomics, and evolution*. Editors F. G. Flores and A. Herrero (Caister Academic Press), 1–19.
- Landfald, B., and Strom, A. R. (1986). Choline-glycine Betaine Pathway Confers a High Level of Osmotic Tolerance in *Escherichia coli*. *J. Bacteriol.* 165, 849–855. doi:10.1128/jb.165.3.849-855.1986
- Leitão, E., Pereira, S., Bondoso, J., Ferreira, D., Pinto, F., Moradasferreira, P., et al. (2006). Genes Involved in the Maturation of Hydrogenase(s) in the

- Nonheterocystous Cyanobacterium *Lyngbya Majuscula* CCAP 1446/4. *Int. J. Hydrogen Energ.* 31, 1469–1477. doi:10.1016/j.ijhydene.2006.06.012
- Lever, M., and Slow, S. (2010). The Clinical Significance of Betaine, an Osmolyte with a Key Role in Methyl Group Metabolism. *Clin. Biochem.* 43, 732–744. doi:10.1016/j.clinbiochem.2010.03.009
- Lindblad, P. (2018). “Hydrogen Production Using Novel Photosynthetic Cell Factories. Cyanobacterial Hydrogen Production: Design of Efficient Organisms,” in *Microalgal Hydrogen Production: Achievements and Perspectives*. Editors G. Torzillo and M. Seibert (UK: G. Royal Society of Chemistry), 323–334.
- Meeks, J. C., and Castenholz, R. W. (1971). Growth and Photosynthesis in an Extreme Thermophile, *Synechococcus lividus* (Cyanophyta). *Archiv. Mikrobiol.* 78, 25–41. doi:10.1007/bf00409086
- Miao, X., Wu, Q., Wu, G., and Zhao, N. (2003). Sucrose Accumulation in Salt-Stressed Cells of *gpp* Gene Deletion-Mutant in cyanobacterium *Synechocystis* sp. PCC 6803. *FEMS Microbiol. Lett.* 218, 71–77. doi:10.1111/j.1574-6968.2003.tb11500.x
- Montagud, A., Navarro, E., Fernández de Córdoba, P., Urchueguía, J. F., and Patil, K. R. (2010). Reconstruction and Analysis of Genome-Scale Metabolic Model of a Photosynthetic Bacterium. *BMC Syst. Biol.* 4, 156. doi:10.1186/1752-0509-4-156
- Montagud, A., Zelezniak, A., Navarro, E., de Córdoba, P. F., Urchueguía, J. F., and Patil, K. R. (2011). Flux Coupling and Transcriptional Regulation within the Metabolic Network of the Photosynthetic Bacterium *Synechocystis* sp. PCC6803. *Biotechnol. J.* 6, 330–342. doi:10.1002/biot.201000109
- Mota, R., Guimarães, R., Büttel, Z., Rossi, F., Colica, G., Silva, C. J., et al. (2013). Production and Characterization of Extracellular Carbohydrate Polymer from *Cyanospora* sp. CCY 0110. *Carbohydr. Polym.* 92, 1408–1415. doi:10.1016/j.carbpol.2012.10.070
- Nsimba, Z. F., Paquot, M., Mvumbi, L. G., and Deleu, M. (2010). Glycine Betaine Surfactant Derivatives: Synthesis Methods and Potentialities of Use. *Biotechnol. Agron. Soc. Environ.* 14, 737–748.
- Nyssonlä, A., Kerovu, J., Kaukinen, P., von Weymarn, N., and Reinikainen, T. (2000). Extreme Halophiles Synthesize Betaine from glycine by Methylation. *J. Biol. Chem.* 275, 22196–22201. doi:10.1074/jbc.m910111199
- Oren, A., Haldal, M., Norland, S., and Galinski, E. (2002). Intracellular Ion and Organic Solute Concentrations of the Extremely Halophilic Bacterium *Salinibacter ruber*. *Extremophiles* 6, 491–498. doi:10.1007/s00792-002-0286-3
- Orth, J. D., Thiele, I., and Palsson, B. Ø. (2010). What Is Flux Balance Analysis? *Nat. Biotechnol.* 28, 245–248. doi:10.1038/nbt.1614
- Pacheco, C. C., Ferreira, E. A., Oliveira, P., and Tamagnini, P. (2021). “Synthetic Biology of Cyanobacteria,” in *The Autotrophic Biorefinery: Raw Materials from Biotechnology*. Editors R. Kourist and S. Schmidt, 131–172. doi:10.1515/9783110550603-006
- Pereira, S. B., Santos, M., Leite, J. P., Flores, C., Eisfeld, C., Büttel, Z., et al. (2019). The Role of the Tyrosine Kinase Wzc (SlI0923) and the Phosphatase Wzb (Slr0328) in the Production of Extracellular Polymeric Substances (EPS) by *Synechocystis* PCC 6803. *Microbiologyopen* 8, e00753. doi:10.1002/mbo3.753
- Pinto, F., Pacheco, C. C., Ferreira, D., Moradas-Ferreira, P., and Tamagnini, P. (2012). Selection of Suitable Reference Genes for RT-qPCR Analyses in Cyanobacteria. *PLoS One* 7, e34983. doi:10.1371/journal.pone.0034983
- Pinto, F., Pacheco, C. C., Oliveira, P., Montagud, A., Landels, A., Couto, N., et al. (2015). Improving a *Synechocystis*-Based Photoautotrophic Chassis through Systematic Genome Mapping and Validation of Neutral Sites. *DNA Res.* 22, 425–437. doi:10.1093/dnares/dsv024
- Rady, M. O. A., Semida, W. M., Abd El-Mageed, T. A., Hemida, K. A., and Rady, M. M. (2018). Up-regulation of Antioxidative Defense Systems by glycine Betaine Foliar Application in Onion Plants Confer Tolerance to Salinity Stress. *Scientia Horticulturae* 240, 614–622. doi:10.1016/j.scienta.2018.06.069
- Rathinasabapathi, B., Burnet, M., Russell, B. L., Gage, D. A., Liao, P.-C., Nye, G. J., et al. (1997). Choline Monooxygenase, an Unusual Iron-Sulfur Enzyme Catalyzing the First Step of glycine Betaine Synthesis in Plants: Prosthetic Group Characterization and cDNA Cloning. *Proc. Natl. Acad. Sci.* 94, 3454–3458. doi:10.1073/pnas.94.7.3454
- Rodrigues, J. S., and Lindberg, P. (2021). “Engineering Cyanobacteria as Host Organisms for Production of Terpenes and Terpenoids,” in *Cyanobacteria Biotechnology*. Editors S. L. Jens Nielsen, G. Stephanopoulos, and P. Hudson (WILEY-VCH GmbH), 267–300. doi:10.1002/9783527824908.ch9
- Sadvakasova, A. K., Kossalbayev, B. D., Zayadan, B. K., Bolatkhan, K., Alwasel, S., Najafpour, M. M., et al. (2020). Bioprocesses of Hydrogen Production by Cyanobacteria Cells and Possible Ways to Increase Their Productivity. *Renew. Sust. Energ. Rev.* 133, 110054. doi:10.1016/j.rser.2020.110054
- Sambrook, J., and Russel, D. (2001). *Molecular Cloning: A Laboratory Manual*. 3rd ed. NY, USA: Cold Spring Harbor Laboratory Press.
- Santos, H., Lamosa, P., and Borges, N. (2006). “Characterization and Quantification of Compatible Solutes in (Hyper)thermophilic Microorganisms,” in *Methods in Microbiology*. Editors F. A. Rainey and A. Oren (Academic Press), 35, 173–199. Extremophiles. doi:10.1016/s0580-9517(08)70011-4
- Schäfer, A., Tauch, A., Jäger, W., Kalinowski, J., Thierbach, G., and Pühler, A. (1994). Small Mobilizable Multi-Purpose Cloning Vectors Derived from the *Escherichia coli* Plasmids pK18 and pK19: Selection of Defined Deletions in the Chromosome of *Corynebacterium glutamicum*. *Gene* 145, 69–73. doi:10.1016/0378-1119(94)90324-7
- Shkryl, Y., Degtyarenko, A., Grigorovich, V., Balabanova, L., and Tekutyeva, L. (2020). Betaine Biosynthesis in a Heterologous Expression System Based on the B12 Producer *Pseudomonas denitrificans*. Paper presented at the E3S Web of Conferences .
- Silva-Rocha, R., Martínez-García, E., Calles, B., Chavarría, M., Arce-Rodríguez, A., de las Heras, A., et al. (2013). The Standard European Vector Architecture (SEVA): a Coherent Platform for the Analysis and Deployment of Complex Prokaryotic Phenotypes. *Nucleic Acids Res.* 41, D666–D675. doi:10.1093/nar/gks1119
- Singh, M., Sharma, N. K., Prasad, S. B., Yadav, S. S., Narayan, G., and Rai, A. K. (2013). The Freshwater Cyanobacterium *Anabaena doliolum* Transformed with *ApGSM-T-DMT* Exhibited Enhanced Salt Tolerance and protection to Nitrogenase Activity, but Became Halophilic. *Microbiol.* 159, 641–648. doi:10.1099/mic.0.065078-0
- Stadmler, S. S., Gorensk-Benitez, A. H., Guseman, A. J., and Pielak, G. J. (2017). Osmotic Shock Induced Protein Destabilization in Living Cells and its Reversal by glycine Betaine. *J. Mol. Biol.* 429, 1155–1161. doi:10.1016/j.jmb.2017.03.001
- Stanier, R. Y., Kunisawa, R., Mandel, M., and Cohen-Bazire, G. (1971). Purification and Properties of Unicellular Blue-green Algae (Order *Chroococcales*). *Bacteriol. Rev.* 35, 171–205. doi:10.1128/br.35.2.171-205.1971
- Sun, H., Luo, M., Zhou, X., Zhou, Q., Sun, Y., Ge, W., et al. (2020). Exogenous glycine Betaine Treatment Alleviates Low Temperature-Induced Pericarp Browning of ‘Nanguo’ Pears by Regulating Antioxidant Enzymes and Proline Metabolism. *Food Chem.* 306, 125626. doi:10.1016/j.foodchem.2019.125626
- Tamagnini, P., Troshina, O., Oxelfelt, F., Salema, R., and Lindblad, P. (1997). Hydrogenases in *Nostoc* sp. Strain PCC 73102, a Strain Lacking a Bidirectional Enzyme. *Appl. Environ. Microbiol.* 63, 1801–1807. doi:10.1128/aem.63.5.1801-1807.1997
- Trautmann, D., Voss, B., Wilde, A., Al-Babili, S., and Hess, W. R. (2012). Microevolution in Cyanobacteria: Re-sequencing a Motile Substrain of *Synechocystis* sp. PCC 6803. *DNA Res.* 19, 435–448. doi:10.1093/dnares/dss024
- Waditee, R., Bhuiyan, M. N. H., Rai, V., Aoki, K., Tanaka, Y., Hibino, T., et al. (2005). Genes for Direct Methylation of glycine Provide High Levels of glycinebetaine and Abiotic-Stress Tolerance in *Synechococcus* and *Arabidopsis*. *Proc. Natl. Acad. Sci.* 102, 1318–1323. doi:10.1073/pnas.0409017102
- Waditee, R., Bhuiyan, N. H., Hirata, E., Hibino, T., Tanaka, Y., Shikata, M., et al. (2007). Metabolic Engineering for Betaine Accumulation in Microbes and Plants. *J. Biol. Chem.* 282, 34185–34193. doi:10.1074/jbc.m704939200
- Waditee, R., Tanaka, Y., Aoki, K., Hibino, T., Jikuya, H., Takano, J., et al. (2003). Isolation and Functional Characterization of N-Methyltransferases that Catalyze Betaine Synthesis from Glycine in a Halotolerant Photosynthetic Organism *Aphanospora halophytica*. *J. Biol. Chem.* 278, 4932–4942. doi:10.1074/jbc.m210970200
- Waditee-Sirisattha, R., Kageyama, H., Fukaya, M., Rai, V., and Takabe, T. (2015). Nitrate and Amino Acid Availability Affects glycine Betaine and Mycosporine-2-glycine in Response to Changes of Salinity in a Halotolerant cyanobacterium *Aphanospora halophytica*. *FEMS Microbiol. Lett.* 362, fnv198. doi:10.1093/femsle/fnv198
- Waditee-Sirisattha, R., Singh, M., Kageyama, H., Sittipol, D., Rai, A. K., and Takabe, T. (2012). *Anabaena* sp. PCC7120 Transformed with glycine Methylation Genes from *Aphanospora Halophytica* Synthesized glycine

- Betaine Showing Increased Tolerance to Salt. *Arch. Microbiol.* 194, 909–914. doi:10.1007/s00203-012-0824-z
- Wang, L., Chen, L., Yang, S., and Tan, X. (2020). Photosynthetic Conversion of Carbon Dioxide to Oleochemicals by Cyanobacteria: Recent Advances and Future Perspectives. *Front. Microbiol.* 11, 634. doi:10.3389/fmicb.2020.00634
- Williams, J. G. K. (1988). [85] Construction of Specific Mutations in Photosystem II Photosynthetic Reaction center by Genetic Engineering Methods in *Synechocystis* 6803. *Methods Enzymol.* 167, 766–778. doi:10.1016/0076-6879(88)67088-1
- Wu, W., Du, W., Gallego, R. P., Hellingwerf, K. J., van der Woude, A. D., and Branco dos Santos, F. (2020). Using Osmotic Stress to Stabilize Mannitol Production in *Synechocystis* sp. PCC6803. *Biotechnol. Biofuels* 13, 117. doi:10.1186/s13068-020-01755-3
- You, L., Song, Q., Wu, Y., Li, S., Jiang, C., Chang, L., et al. (2019). Accumulation of glycine Betaine in Transplastomic Potato Plants Expressing Choline Oxidase Confers Improved Drought Tolerance. *Planta* 249, 1963–1975. doi:10.1007/s00425-019-03132-3
- Conflict of Interest:** The authors declare that the research was conducted in the absence of any commercial or financial relationships that could be construed as a potential conflict of interest.
- Publisher's Note:** All claims expressed in this article are solely those of the authors and do not necessarily represent those of their affiliated organizations, or those of the publisher, the editors and the reviewers. Any product that may be evaluated in this article, or claim that may be made by its manufacturer, is not guaranteed or endorsed by the publisher.
- Copyright © 2022 Ferreira, Pacheco, Rodrigues, Pinto, Lamosa, Fuente, Urchueguía and Tamagnini. This is an open-access article distributed under the terms of the Creative Commons Attribution License (CC BY). The use, distribution or reproduction in other forums is permitted, provided the original author(s) and the copyright owner(s) are credited and that the original publication in this journal is cited, in accordance with accepted academic practice. No use, distribution or reproduction is permitted which does not comply with these terms.